28/01/2018

Dear editor, we are pleasant to present the revised version of the paper "Hydrological control of large hurricane-induced lahars: evidences from rainfall-runoff modelling, seismic and video monitoring." by Capra et al. We consider that the revised version benefits from the constructive revisions of three reviewer and one comment. We followed all the suggestions made. Here below you will find the responses to all the points raised in the revisions, and main changes consisted in:

- The English was revised based on the reviewer suggestions.
- The Green-Ampt infiltration model was added to discuss the limitation of the SCS-NC method and validate the simulations. Based on this, section 2.4. is now improved and a new figure (4) was added.
- The rainfall data as input parameter for simulation is now better described, and Figure 3 was modified adding a new graph showing the rainfall behavior at two different rain gauges for the Jova and Patricia events.
- Figure 8 (now Figure 9) was modified as suggested.

Here below detailed responses to each comment are provided. The marked-up manuscript version is added at the end of this document.

On behalf of my coauthors.

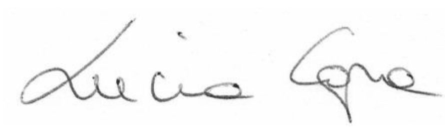

Lucia Capra

Responses to SC1.

We would like to thank the reviewer for the comments and constructive suggestions made to improve the present work. Please find below the reviewer's comment and authors' replies to these comments.

The paper of Lucia Capra and her colleagues provides a valuable contribution to the analysis of the relationships between flood runoff formation and lahar occurrence during hurricanes. Lahar monitoring and characterization of hydraulic properties of soils in a difficult environment deserve to be stressed. The aim of this note is to propose some comments on specific aspects of the analysis.

The core of the study is the assessment of the runoff response to hurricanes and the comparison of simulated flood hydrographs with the monitored lahars. Since no measurements of water discharge are available in the studied catchments, rainfall-runoff modeling (this term should be preferred to "rainfall simulation") remains essentially uncalibrated. It is well-known that a careful selection of model parameters does not ensure a satisfactory correspondence between simulated and real hydrographs. The lack of rainfall-runoff model calibration and the impossibility of performing it in the studied catchments should be acknowledged and discussed. More could be said, moreover, about the propagation of rainfall excess computed by means of the SCS Curve Number method: this part of runoff simulation is of utmost importance for the timing of flood response. A sensitivity analysis on rainfall-runoff model parameters, although does not surrogate model calibration, could help coping with the uncertainties in the assessment of flood response.

The impossibility of calibrating rainfall-runoff models is the reason why simulated water flood hydrographs have seldom been compared with observed debris flow hydrographs in catchments instrumented for debris flow monitoring.

A possible, even if only partial, check of model results with the observed runoff response could consist in the comparison of the time of the first rise of the simulated hydrograph with video images showing the onset of the water flood at the monitoring stations. According to figure 8, this comparison could be possible for Hurricane Manuel at Montegrande (Fig. 8b) and Hurricane Patricia at La Lumbre (Fig. 8d), whereas the early occurrence of lahars prevents it in the other two cases (Figs. 8a and 8c).

We perfectly agree with the reviewer. As pointed out, no measurements of water discharge are available at both La Lumbre and Montegrande watershed, so a model calibration is not possible. We followed the suggestion by L. Marchi and we calibrated the simulated watershed discharge using the information gathered from video images acquired by the monitoring station of La Lumbre ravine during the Patricia event. For Montegrande ravine a calibration would be possible only for the 11 June 2013 event, but considering the strong effect of soil hydrophobicity at the beginning of the rainy season it is difficult to set up a comparison.

For the new version of the manuscript, a rainfall-runoff modeling was performed with both SCS-CN and Green-Ampt (G-A) methods. We decided to also run the simulations with the G-A infiltration method to discuss the limitation of the SCS-CN that does not consider the rainfall intensity (for more detail see response to RC2). The simulated watershed discharge obtained with the G-A method best fits with the initial shallow-water flow observed in the video images, however, main peaks discharges corresponding with the main lahars pulses are equally reproduced with both infiltration models (see new figure R1 at the end of this document). Based on this result, and considering the limited number of parameters needed to apply the SCS-CN method, we focused on the latter method that would be more suitable to adopt in an early warning system devoted to forecast the lag time of main lahar pulses at a specific site. We improved and modified the section "2.4. Rainfall-runoff modelling" as follows (see also response to RC2). Other authors already performed a sensitive analysis of the G-A method, showing that the saturated hydraulic conductivity Ks is a key factor in the estimation of infiltration rates and exerts a notable influence on runoff calculations (i.e. Chen et al., 2015). With respect to the SCS-CN model, the only input parameter is the Curve Number, thus we present a simple comparison for Patricia event at La Lumbre ravine. Results obtained with the 80/75 CN values for channel and vegetated area respectively are compared with two other simulations performed using global values of 75 and 80 (see table R2). This exercise shows that the uncertainty in simulated maximum peak discharge is in the range of 0.1 hr, pointing that a global CN value could be also used for the Volcán de Colima.

Table R1

Parameter used in the G-A simulations	
Abstraction	6 (mm)
Ks	20 (mm/hr)
soil-suction	100 (mm)
initial saturation	0.1
final saturation	0.35

Table R2. SCS-CN simulations with different CNs

Surges observed in the images	**peak III (23.5 hr)**	**peak IV (24 hr)**
CN	*time in the simulated watershed discharge curve*	
75 global	*23.4*	***24.1***
80/75 (channel/vegetated)	***23.5***	***24.1***
80 global	***23.5***	*24.2*

2.4. Rainfall-runoff modelling

To better understand the lahar behavior and duration during extreme hydrometeorological events at Volcán de Colima, rainfall-runoff simulations were performed with Flo-2D code (O´Brian et al., 1993). The Flo-2D code routes the overland flow as discretized shallow sheet flow using the Green-Ampt or the SCS Curve number (or combined) infiltration models. For the present work, the SCS Curve Number (SCS-CN, i.e. Mishra and Singh, 2003) was selected but a comparison between both infiltration models is presented below. The rainfall is applied to the entire watershed, without spatial variability as we are dealing with large-scale, long-duration hurricane-induced rainfall. This rainfall is discretized as a cumulative percent of the total precipitation each 10 minutes. With the SCS-CN model, the volume of water runoff produced by the simulated precipitation is estimated through the use of a single parameter, i.e. the Curve Number (CN). This parameter summarizes the influence of both the superficial and deep soil features, including the saturated hydraulic conductivity, type of land use, and humidity before the precipitation event (for an accurate description of the origin of the method see Rallison, 1980; Ponce and Hawkins, 1996). A similar approach was previously used for modeling debris flow initiation mechanisms (i.e. Gentile et al., 2006; Llanes et al., 2015). To apply the SCS-CN model, it is necessary to classify the soil in one of four groups, each identifying a different potential runoff generation (A, B, C, D; USDA-NRCS 2007). La Lumbre and Montegrande watersheds were subdivided into two main zones: 1) the unvegetated upper cone and the main channel, that consists of unconsolidated pyroclastic material with large boulders embedded in a sandy to silty matrix, and 2) the vegetated lateral terraces, composed by old pyroclastic sequences with incipient soils and are vegetated with pine trees and sparse bushes. Based on these observations, soils were classified between group A and B (Bartolini and Borselli, 2009). CN for the vegetated terraces and for the nude soils is estimated at 75 and 80 respectively (in wet season, Hawkins et al., 1985; Ferrer-Julia et al. 2003). To perform a simulation with the FLO-2D code, two polygons were traced to delimit the un-vegetated portion of the cone from the vegetated area of the watershed, and at each polygon the relative CN value was assigned. At the apex of each watershed a barrier of outflow points were defined to obtain the values of the simulated watershed discharge computed at each 0.1 hr. The simulation was performed with a 20-m digital elevation model. One of the limitations of the SCS-CN model is that it does not consider the effect of the rainfall intensity on the infiltration. In addition, since no measurements of water discharge are available at both La Lumbre and Montegrande basins, it is difficult to calibrate the simulations here presented. To investigate the SCS-CN model uncertainties in the assessment of flood response, the Green-Ampt (1911) model (G-A), sensitive to the rainfall intensity, was also applied and results were compared with the outcome of SCS-CN model. For the G-A method, the main input parameters are the saturated hydraulic conductivity (Ks), the soil suction and the volumetric moisture deficiency. Ks is the key factor in the estimation of infiltration rates and exerts a notable influence on runoff calculations, therefore it requires great care in its measurement (Grimaldi et al., 2013). These values can be extrapolated from reference tables or directly measured with field experiments. Based on the textural characteristics of soils at Volcán de Colima as well as type of vegetation, input parameters were selected from the FLO-2D reference manual. In particular, with a value of Ks of 20 mm/hr the simulated watershed discharge best fits with the precursory shallow-water flow observed in the video images, as it will be showed below (Figure R1). The Ks value of 20 mm/hr is equivalent to the CN value used for the SCS-NC simulation. In fact an empirical relation between Ks and CN has been proposed be Chong and Teng (1986):

$$S = 3.579Ks^{1.208}$$

where S is the potential retention and it is related to the CN as follow (Mockus, 1972):

$$CN = \frac{2540}{S + 25.4}$$

Based on these equations, a value of Ks equal to 20 mm/hr corresponds to a CN of 75.5 in the range of values here used for the SCS-NC infiltration model.

The G-A infiltration model was tested at La Lumbre ravine, using the Patricia rainfall and comparing the simulated watershed discharge curve with the available video images. Figure R1 shows the discharge curve that best fits with the data gathered from the images (Table #), based on which the two method were qualitative calibrated. The G-A infiltration model nicely reproduce the initial scouring of a muddy water and it corresponds with the first increase in the simulated watershed discharge. The SCS-CN infiltration model is not able to reproduce this first water runoff. This can be explained considering that the initial abstraction due to the interception, infiltration and surface storage, is automatically computed in the SCS-NC model as 0.2S, being probably too high for the studied area. In contrast, with the G-A method, the initial abstraction can be modified and best results were obtained with a value of 6 mm that corresponds to a surface typical of a vegetated mountain region (Table #). However, both infiltration models give similar results for the main peaks of the simulated maximum watershed discharge that correspond with the arrival of the main lahar pulses as observed from the image (Figure R1). These results show that the G-A model is much more reliable to detect precursory slurry flows, while both models are equally able to catch the main surges of a lahar. One important point is that the simulations are here used to set up an early warning system to forecast the lag time of the main lahar surges. The first slurry flows were here important to calibrate the G-A simulation but they do not represent an essential data for the early warning system. In addition, input data for the G-A method often are difficult to set, requiring great care in its measurement; in contrast, the output of the SCS-CN method only depends on the CN value. The SCS-CN method has been largely used in rainfall-runoff modeling, and we consider that is a valuable method for the objective of the present work, as we are not seeking for a quantitative estimation of the watershed discharge but on the arrival time of the main lahar pulses.

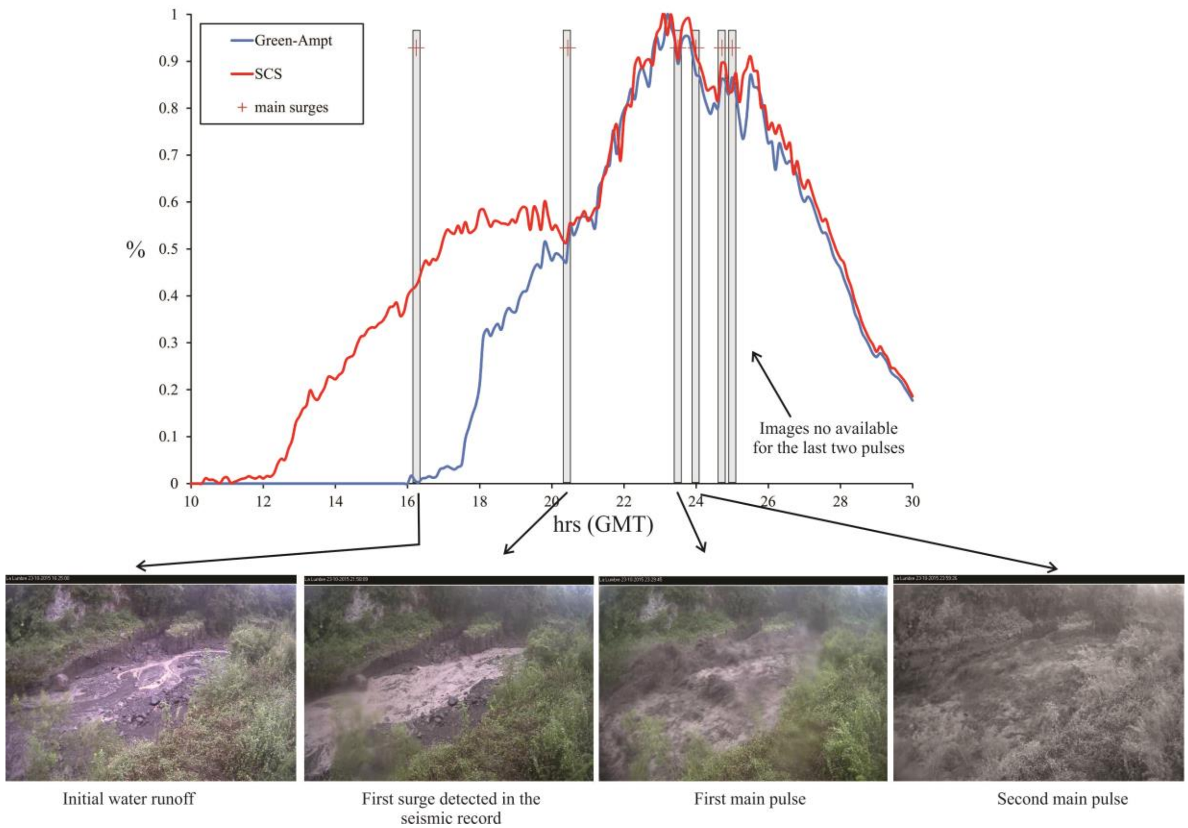

Figure R1. Comparison of simulated watershed discharge curves based on SCS-NC and G-A infiltration models. Qualitative calibration is here proposed based on the flow discharge as observed at the MSL site.

Response to RC1.

We would like to thank the reviewer for the comments and constructive suggestions made to improve the present work. Please find below the reviewer's comment and authors' replies to these comments.

The paper provides an interesting study about the relationship between the rain induced by hurricanes and the generation of lahars. The paper mostly requires an English grammar revision. Nevertheless, I suggest that as the Coulomb failure criterion was not mentioned in the paper, to include it within the paper, perhaps when the authors mention landslide triggering empiric criterion (section Discussion).

We consider that the Coulomb failure criterion is out of the focus of the present paper, we are not discussing the condition of lahar initiation; lahars at Volcan de Colima originate from a progressive erosion of material from the river bed.

It draws attention that in the abstract, numerical modeling of rain and infiltration is promised. None of them are fulfilled. The O'Brian model is a shallow water approach for surface flows, despite the claim done by the authors within the paper that it was used for rain fall modeling.

We agree with the reviewer and we were wrongly using the terminology, in fact the paper presents rainfall-runoff simulations, as also point out by the SC1.

In addition, there are few more suggestions listed below.

We took into account of the following suggestions. The English revision was based on the suggestions made by RC2 and SC2.

1 Abstract
Review English
2 Methods and data
1. line 132: use primary source (Gravelius, 1914)
done
2. line 175. Review English.
3. Line 224: Mistake, the aim of Flo2D is not to do rainfall simulations.
Changed to rainfall-runoff simulation
4. Line 228: clarify how do you simulated the precipitation.
This is now clarified as follow.
The rainfall is applied to the entire watershed, without a spatial variation, and it is discretized as a cumulative percent of the total precipitation each 10 minutes.
5. Line 235: zones
done
3 Results
1. Line 278, figure 5: keep the previously used convention for the sub-figure numbering (top left hand side).
done
8. Line 400: if actually "it could have been possible" , why it was not possible? It is always risky to extrapolate, thus to advise extrapolations.

This refers that if at the time of Patricia event this model was ready, the simulation could have been run to have a forecast of the arrival times of the main lahar surges. The text was slightly modified as follow

For the 2015 Hurricane Patricia event the weather forecast predicted an estimated value for the total rainfall, and also the approximate time of its landfall. Based on the deigned storm obtained with the rainfall/time distribution of the analyzed events, it would have been possible to anticipate when lahars started along the La Lumbre ravine, and the arrival time of main pulses. Then, this first prediction could be constrained using rainfall-runoff modeling based on real-time monitoring data, as simulations do not take more than 30 minutes to run.

Responses to RC2
We would like to thank the reviewer for the comments and constructive suggestions made to improve the present work. Please find below the reviewer's comment and authors' replies to these comments.

Main issues

As mentioned above, the rainfall simulations used in this work need to be clarified and care needs to be taken when analysing and drawing conclusions from the simulation results. In particular:

1. **What are the assumptions of the SCS curve model and how may it affect results?**

The SCS approach is a simplified method for estimating rainfall runoff. Lower curve numbers result in less runoff for the same amount of rainfall. However, as stated on lines 229-231, this model simplifies the complex relationship between rainfall and overland flow into a single number. A weakness of this approach is that the curve number does not consider the effects of single storm properties (e.g. rainfall intensity) on infiltration.

We agree with the reviewer that SCS-NC method does not consider the effect of the rainfall intensity on infiltration, a key point for the cases here analyzed. But it is worth mentioning that here the rainfall input for the FLO-2D simulation is given as a no-linear hydrograph curve where accumulated rainfall is discretized at each 10 minutes interval (as detected with the raingauge). Based also on the comment by L. Marchi (SC1), we tested the Green-Ampt (G-A) rainfall-infiltration method and we calibrated it with the images available for the Patricia event along the La Lumbre ravine, at least for the arrival time of the first slurry flow and for the main surges (this last correlation was already presented in fig.8). The parameters used for the Green-Ampt method were selected from FLO-2D reference tables according to the textural characteristics of the soil on the watershed (Table R1). The Ks (saturated hydraulic conductivity) of 20 mm/hr gives the best fit, and based on the equation proposed by Chong and Teng (1986) it corresponds to a CN of 75.5 in the range of the value used for the simulation performed with the SCS-NC method (see detailed explanation in the text below). It is worth to mention that the input parameters here used for the G-A model represent an average value for the entire watershed

Table R1

Parameter used in the G-A simulations	
Abstraction	6 (mm)
Ks	20 (mm/hr)
soil-suction	100 (mm)
initial saturation	0.1
final saturation	0.35

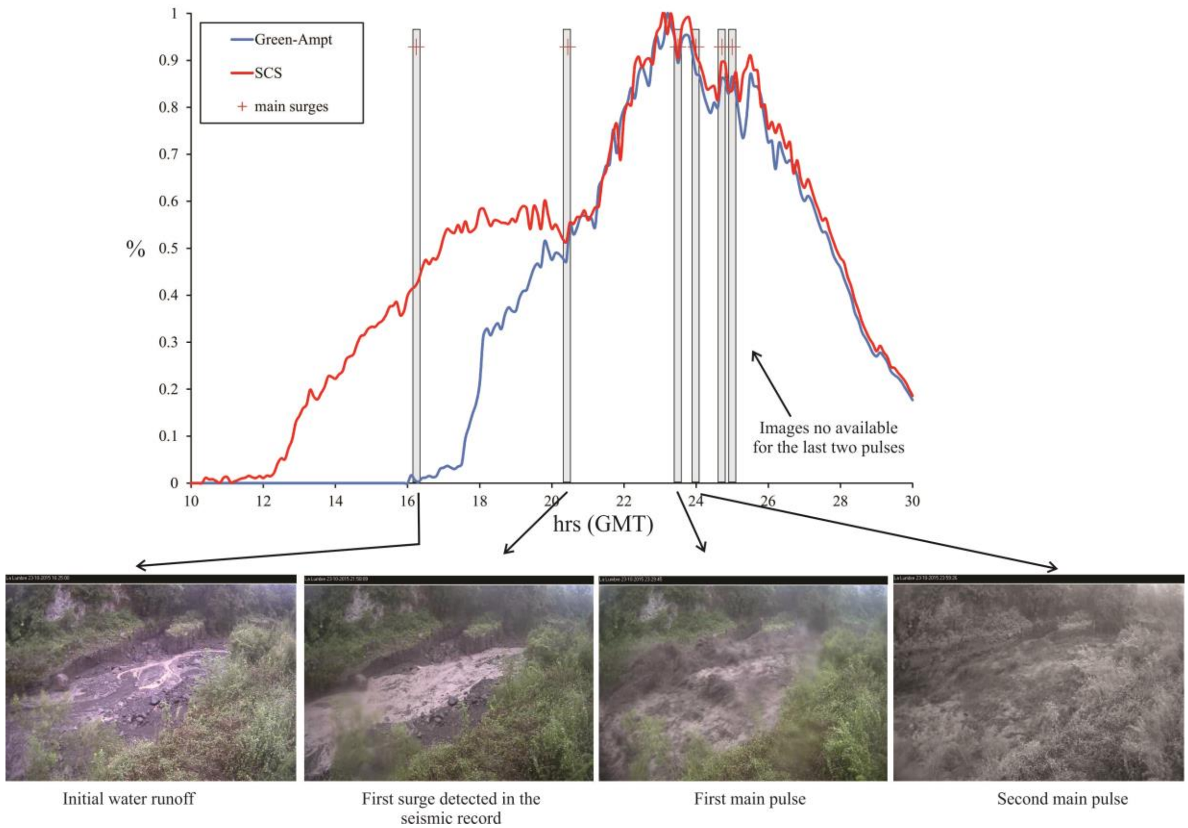

Figure R1. Comparison of simulated watershed discharge curves based on SCS-NC and G-A infiltration models. Qualitative calibration is here proposed based on the flow discharge as observed at the MSL site.

Figure R1 shows the comparison of the discharge curve obtained with the SCS and G-A methods and their comparison with selected images of the flow along the La Lumbre channel during the Patricia event.

One first issue is the coincidence of the first water runoff along the channel observed in the image with the rise of the discharge in the curve modeled with G-A method, as the SCS-CN is not able to reproduce it. In fact, we performed additional simulation to try to reproduce the initial slurry flow with the SCS method but it was impossible. This can be explained considering that the model automatically assumes an initial abstraction (rainfall intercepted by vegetation) of 0.2S, where S is the potential retention included in the CN calculation (CN=2540/(S+25.4) (Mockus, 1972), value that it is too high for the studied area. In contrast, the value of initial abstraction can be controlled performing the simulations with the G-A method. However, the main peak discharges corresponding with the main lahar pulses are equally reproduced with both models. Under this evidence, we are able to affirm that the G-A method is much more reliable to detect the first streamflow, but the SCS method is also able to catch the main surges. One important point is that the simulations are here used to set up an early warning system to forecast the lag time of main lahar pulses at a specific site. The first water runoff along the channel was fundamental to calibrate the G-A simulation but it is not an essential data for the early warning system. In addition, input data for the G-A method are probably much more difficult to set, in contrast to the SCS method where only one parameter is needed. A new section has been added within the paragraph "**2.4.**

Rainfall-runoff modeling” to show the comparison between the two infiltration methods based on which the SCS model was selected to be used in the early warning system. The SCS method has been largely used in rainfall-runoff estimations, and we consider that is a valuable method for the objective of the present work. This section was modified as follow:

2.4. Rainfall-runoff modelling

To better understand the lahar behavior and duration during extreme hydrometeorological events at Volcán de Colima, rainfall-runoff simulations were performed with Flo-2D code (O´Brian et al., 1993). The Flo-2D code routes the overland flow as discretized shallow sheet flow using the Green-Ampt or the SCS Curve number (or combined) infiltration models. For the present work, the SCS Curve Number (SCS-CN, i.e. Mishra and Singh, 2003) was selected but a comparison between both infiltration models is presented below. The rainfall is applied to the entire watershed, without spatial variability as we are dealing with large-scale, long-duration hurricane-induced rainfall. This rainfall is discretized as a cumulative percent of the total precipitation each 10 minutes. With the SCS-CN model, the volume of water runoff produced by the simulated precipitation is estimated through the use of a single parameter, i.e. the Curve Number (CN). This parameter summarizes the influence of both the superficial and deep soil features, including the saturated hydraulic conductivity, type of land use, and humidity before the precipitation event (for an accurate description of the origin of the method see Rallison, 1980; Ponce and Hawkins, 1996). A similar approach was previously used for modeling debris flow initiation mechanisms (i.e. Gentile et al., 2006; Llanes et al., 2015). To apply the SCS-CN model, it is necessary to classify the soil in one of four groups, each identifying a different potential runoff generation (A, B, C, D; USDA-NRCS 2007). La Lumbre and Montegrande watersheds were subdivided into two main zones: 1) the unvegetated upper cone and the main channel, that consists of unconsolidated pyroclastic material with large boulders embedded in a sandy to silty matrix, and 2) the vegetated lateral terraces, composed by old pyroclastic sequences with incipient soils and are vegetated with pine trees and sparse bushes. Based on these observations, soils were classified between group A and B (Bartolini and Borselli, 2009). CN for the vegetated terraces and for the nude soils is estimated at 75 and 80 respectively (in wet season, Hawkins et al., 1985; Ferrer-Julia et al. 2003). To perform a simulation with the FLO-2D code, two polygons were traced to delimit the un-vegetated portion of the cone from the vegetated area of the watershed, and at each polygon the relative CN value was assigned. At the apex of each watershed a barrier of outflow points were defined to obtain the values of the simulated watershed discharge computed at each 0.1 hr. The simulation was performed with a 20-m digital elevation model. One of the limitations of the SCS-CN model is that it does not consider the effect of the rainfall intensity on the infiltration. In addition, since no measurements of water discharge are available at both La Lumbre and Montegrande basins, it is difficult to calibrate the simulations here presented. To investigate the SCS-CN model uncertainties in the assessment of flood response, the Green-Ampt (1911) model (G-A), sensitive to the rainfall intensity, was also applied and results were compared with the outcome of SCS-CN model. For the G-A method, the main input parameters are the saturated hydraulic conductivity (Ks), the soil suction and the volumetric moisture deficiency. Ks is the key factor in the estimation of infiltration rates and exerts a notable influence on runoff calculations, therefore it requires great care in its measurement (Grimaldi et al., 2013). These values can be extrapolated from reference *tables or directly measured with field experiments. Based on the textural characteristics of soils at Volcán de Colima as well as type of vegetation, input parameters were selected from the FLO-2D reference manual. In particular, with a value of Ks of 20 mm/hr the simulated watershed discharge best fits with the precursory shallow-water flow observed in the video images, as it will be showed below (Figure R1). The Ks value of 20 mm/hr is equivalent to the CN value used for the SCS-NC simulation. In fact an empirical relation between Ks and CN has been proposed be Chong and Teng (1986):*

$$S = 3.579Ks^{1.208}$$

where S is the potential retention and it is related to the CN as follow (Mockus, 1972):

$$CN = \frac{2540}{S + 25.4}$$

Based on these equations, a value of Ks equal to 20 mm/hr corresponds to a CN of 75.5 in the range of values here used for the SCS-NC infiltration model.

The G-A infiltration model was tested at La Lumbre ravine, using the Patricia rainfall and comparing the simulated watershed discharge curve with the available video images. Figure R1 shows the discharge curve that best fits with the data gathered from the images, based on which the two method were qualitative calibrated. The G-A infiltration model nicely reproduce the initial scouring of a muddy water and it corresponds with the first increase in the simulated watershed discharge. The SCS-CN infiltration model is not able to reproduce this first water runoff. This can be explained considering that the initial abstraction due to the interception, infiltration and surface storage, is automatically computed in the SCS-NC model as 0.2S, being probably too high for the studied area. In contrast, with the G-A method, the initial abstraction can be modified and best results were obtained with a value of 6 mm that corresponds to a surface typical of a vegetated mountain region. However, both infiltration models give similar results for the main peaks of the simulated maximum watershed discharge that correspond with the arrival of the main lahar pulses as observed from the image (Figure R1). These results show that the G-A model is much more reliable to detect precursory slurry flows, while both models are equally able to catch the main surges of a lahar. One important point is that the simulations are here used to set up an early warning system to forecast the lag time of the main lahar surges. The first slurry flows were here important to calibrate the G-A simulation but they do not represent an essential data for the early warning system. In addition, input data for the G-A method often are difficult to set, requiring great care in its measurement; in contrast, the output of the SCS-CN method only depends on the CN value. The SCS-CN method has been largely used in rainfall-runoff modeling, and we consider that is a valuable method for the objective of the present work, as we are not seeking for a quantitative estimation of the watershed discharge but on the arrival time of the main lahar pulses.

2. **How was rainfall applied over the simulation domain?**
The authors state that the rainfall 10 minute intervals were applied to the simulation (lines 249-50). However, there is no indication if this varied spatially. If a spatially homogeneous rainfall input was used, the authors need to indicate this and, in discussion, consider the effect

of this assumption on results and implication for the migratory, long duration rainfall scenarios.

The rainfall was applied to the entire watershed, no spatial variation was assumed. As stated before, the total amount of accumulated rainfall is discretized in 10 minutes interval, introduced in the code as a no-linear hydrograph. During tropical rainfalls rains are nearly stationary on top of the volcano. This can be observed by comparing rainfall data from different stations (fig R2). This figure will be added as extra panel in figure 3.

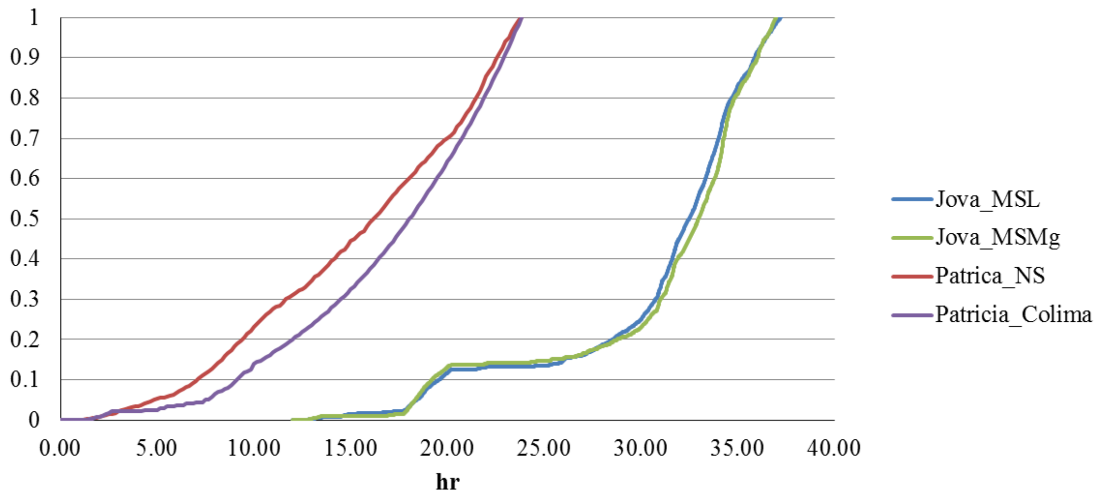

Fig. R2. Normalized rainfall of the Jova and Patricia events as gathered from different stations, pointing to a quasi-stationary rainfall behavior.

3. Related to point 1, in Fig. 8, simulated discharge shows better correlation to identified lahar pulses during Hurricanes Jova, Manuel and Patricia. In these events, rainfall intensity is much lower and cumulative rainfall is more linear than the 11 June event. This highlights a potential limitation of the runoff erosion model that needs to be identified and discussed.

The 11 June 2013 event is presented to stress the fact that at the beginning of the rains season no-stationary, orographic events trigger lahars after few minutes of accumulated rainfall (~10 mm); in those cases, main pulses are clearly controlled by rainfall peak intensities, mainly because of a strong hydrophobic effect of the soils (see Capra et al., 2010). Therefore, the model here presented does not work for such type of events and can be only used during tropical rains associated to hurricanes, with low rainfall intensities and long durations. This concept is clearly stated in the discussion:

This model is strictly related to long-duration and large-scale rainfall events hitting tropical volcanoes such as the Volcán de Colima. In contrast, during mesoscale non-stationary rainfalls, typical at the beginning of the rainy season, lahars are usually triggered at low accumulated rainfall values and manly controlled by rainfall intensity due to the hydrophobic behavior of soils, and they usually consist of single-pulse events with one block-rich front that last less than one hour (i.e. Vázquez et al., 2016b). In perspective, the results presented here can be used to design an Early Warning System (EWS) for hurricane-induced lahars, i.e. event triggered by long-duration and large-scale rainfalls.

4. Although correlation between observed lahar pulses and simulated discharge indicate a level of agreement between simulation and reality, the models have not been calibrated to real world (i.e. measured discharge) data. In effect, the model can then only indicate differences in watershed response between the Montegrade and La Lumbre catchments. Based on these issues, elements of the discussion and conclusion may need modification:

We totally agree. However, based on the calibration presented in the new section we consider that the model here used is reliable. Yes, Montegrande and La Lumbre have a different watershed response, which clearly controls the arrival time of the main lahar pulses that can be simulated with the rainfall-runoff modeling here proposed.

Line 338: pulses better match simulated watershed discharge. This is a crucial distinction, as without calibration we cannot estimate the potential error in the discharge rate.

Again, we think that this aspect is now better justified with the new information based on the comparison between G-A and SCS methods.

Line 338-340: "Nevertheless ...", in Fig. 8c, only one of the four observed pulses coincide with the simulated discharge - this correlation could be (in my opinion likely is) pure coincidence for this event - you need to account for this. I would recommend removing this sentence entirely, as it is largely repeated in lines 357-359.

As stated into the test the 11 June 2013 event does not fit with the model here proposed, but apparently only the last largest pulse correspond with the simulated watershed discharge.

Line 368-371: "This is a well documented mechanism ..." it is hard to interpret what is being said here. What is the difference between discharge rate and watershed discharge? How does one control the other? Rainfall intensity and watershed shape seem to control the arrival of main pulses more than discharge.

We agree we the reviewer and we simplified this section as follow.

Based on data presented here, formation of pulses within a lahar is mostly controlled by the watershed shape that regulates the timing of the arrival of main pulses, depending on the rainfall behavior. Nevertheless, the last pulse is always the largest in volume.

Overall, I suggest to the authors that the strength of this manuscript is in the correlations of multiple streams of data (rainfall intensity, cumulative rain, geophone records) to examine the relationship between rainfall and lahar pulses. Since the rainfall simulations are uncalibrated, they add some context to the discussion, but simulation results (in their current form) cannot be used to draw conclusions about the relationship. I believe the manuscript would be greatly improved by a rewording of the discussion,
reducing the emphasis on rainfall simulations and instead focusing on the relationship between rainfall characteristics and lahar pulses.

Base on the reviewers' comments and the comparison between the SC-NC and G-A infiltration models, we consider that at present our model is much more well justified. Simulations represent an important issue for the present work and, as proposed here, they can be used to perform an early warning system at least to determine the time arrivals of main lahars pulses.

Technical and minor issues

Please see the attached .pdf for corrections to English style and grammar.

All the suggestion to English style and grammar were taken into account.

Line 38, 160, 219: What is a 'stormwater'? This is unclear terminology

This expression was changed to "theoretical rainfall distribution curve"

Line 58: Ruapehu is not in a tropical region.

It was also observed by SC", so this example was removed

Line 161, 165, 170/Figure 1: "MgMS" do you mean MSMg?

Yes, it is now corrected.

Line 163/Figure 1: "LMS" do you mean MSL?

Yes, now corrected

Line 193/194: Change to "Volcán de Colima"

Done

Line 202/203: "Sierra Madre Occidental high relieves" perhaps just Sierra Madre Occidntal range?

Also based to the SC2 reviewer, the sentence was changes.

The system began to develop on 18 October over the Pacific Ocean, strengthened into a hurricane shortly after 00:00 GMT on 22 October and early on 23 October it reached its maximum category of 5, before losing strength as it moved onto the Sierra Madre Occidental range.

Line 225: Reference is O'Brien et al.

Done

Line 317-318 and 320: See above discussion, I think it is important to state the pulses match with peak simulated discharge.

Also based on SR2, the text was clarified.

Line 322-324: Given model assumptions and disparities when compared to the other events, there is a high chance this correlation is coincidental. If you want to note the correlation here, you should also highlight the disparity.

We consider that as already stated into the text, the 11 june 2013 event is here reported only to show the different watershed response at the beginning of the rain season. The model here proposed will be not used to predict the arrival of main pulses for the events at the beginning of the rain season.

Line 333-335: Reword sentence to fix grammar... Seismic and visual data from events analysed here provide evidence to key factors...

Also based on SC2 comment, the sentence was changes as follow:

Based on the seismic and visual data gathered from the events analyzed here, it is possible to identify the key factors in controlling the arrival timing of main lahar fronts.

Line 338-380 and 357-359: See above, these two sentences are almost exactly the

same. Recommend removing the first instance.
We agree and 338-380 lines were deleted.

Line 398-399: "Based on the deigned storm obtained..." meaning is unclear, be specific on the requirements to anticipate start time and arrival of lahar pulses.

For the 2015 Hurricane Patricia event the weather forecast predicted an estimated value for the total rainfall, and also the approximate time of its landfall. Based on the deigned storm obtained with the rainfall/time distribution of the analyzed events, it would have been possible to anticipate when lahars started along the La Lumbre ravine, and the arrival time of main pulses. Then, this first prediction could be constrained using rainfall-runoff modeling based on real-time monitoring data, as simulations do not take more than 30 minutes to run.

Fig. 1 caption: "...locations of the monitoring stations are indicated by triangles"
Done

Fig. 1: Is station MSMg_2015 identified in the manuscript? If not, remove.
The station is now included into the text.

Fig. 3b/c: As a normalised plot, there is no need for the 'y' (norm) axis to be greater than one. Adjust to be between 0 and 1.
Done

Fig. 5c is unnecessary, remove.
Done

Fig. 8 needs to be improved, suggest the following:
- In the caption, rain intensity is a gray line, but in the figure it is gold/yellow.
- Fig. 8b - "Rain" and "Rain intensity" legend entries are switched
- Left axis (%norm) should only be between 0 and 1 (see above)
- Arrows in Fig. 8c do not seem to indicate anything - should "first stream flows" text be placed nearby?
- Color and line choice makes it hard to discriminate between rain intensity and discharge. Try adjust colors or line thicknesses.

Figure was improved as suggested (see next page)

Table 1: The manuscript suggested 'Jova' had seismic records for Montegrade ravine?
Yes, corrected.

Please also note the supplement to this comment:
https://www.nat-hazards-earth-syst-sci-discuss.net/nhess-2017-354/nhess-2017-354-RC2-supplement.pdf

All suggested changes were done

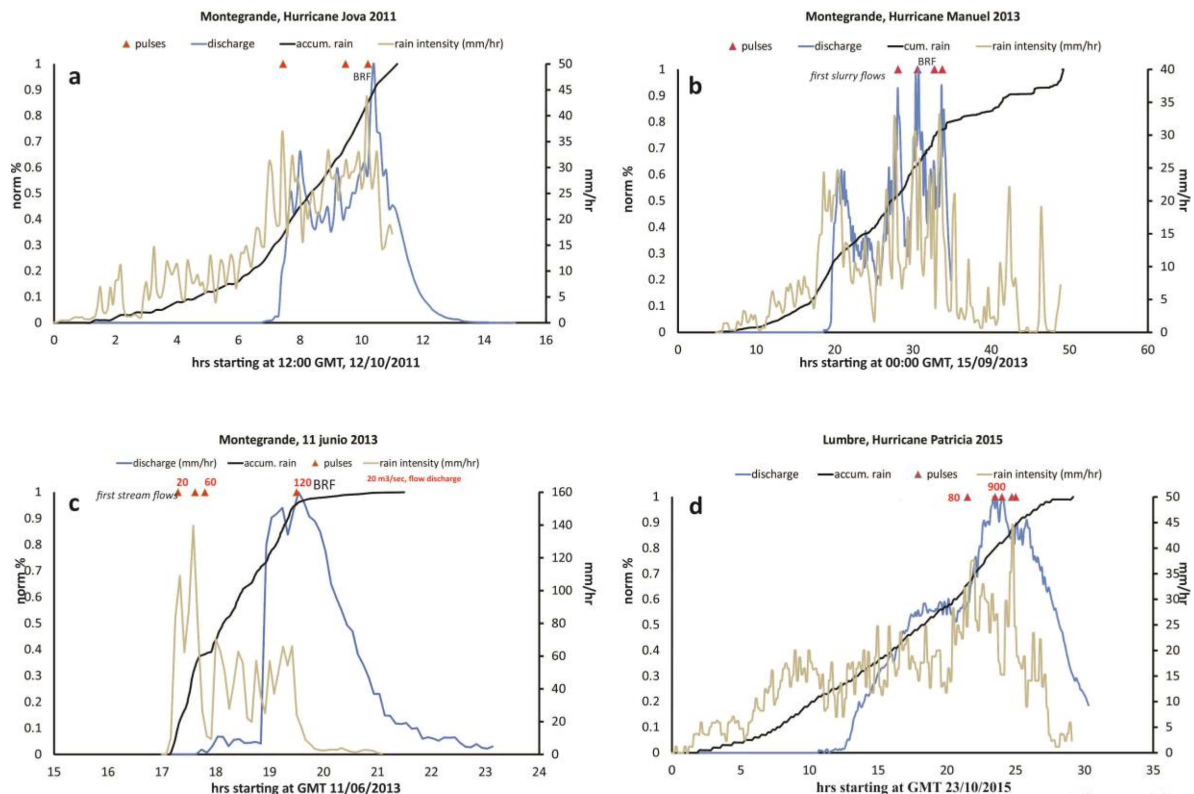

Figure 08

Responses to V. Manville SC2

We would like to thank the reviewer for the comments and constructive suggestions made to improve the present work. Please find below the reviewer's comment and authors' replies to these comments.

Title. The reviewer suggests to mention rainfall-runoff simulation into the title.

We agree and we modified it as follow:
"Hydrological control of large hurricane-induced lahars: evidences from ***rainfall-runoff modellin,*** *seismic and video monitoring"*

1(line 31). How do you define lahar size? By peak discharge, and if so where? Or by peak seismic amplitude by using this as a proxy for lahar volumetric discharge, even though the seismic energy output of a lahar is a function of many factors including volumetric discharge, sediment concentration and sediment grain-size distribution.

Yes, we used the **amplitude as a proxy for lahar volumetric discharge.** On previous published works at Volcán de Colima (Vazquez et al., 2016), the size of lahars has been classified based on their seismic response (amplitude, validated with image data) and duration. With available images, the maximum pick discharge was calculated and assigned to the maximum amplitude recorded form the seismic station. We agree that it is not always possible to correlate the amplitude of the seismic signal with the flow depth, but based on real time data gathered at Colima, there is a quite good correlation for those large events (See. Fig. 5 Vazquez et al., 2016). The figure below extracted from Vazquez et al., 2016, clearly point to a correlation between lahar amplitude and flow discharge.

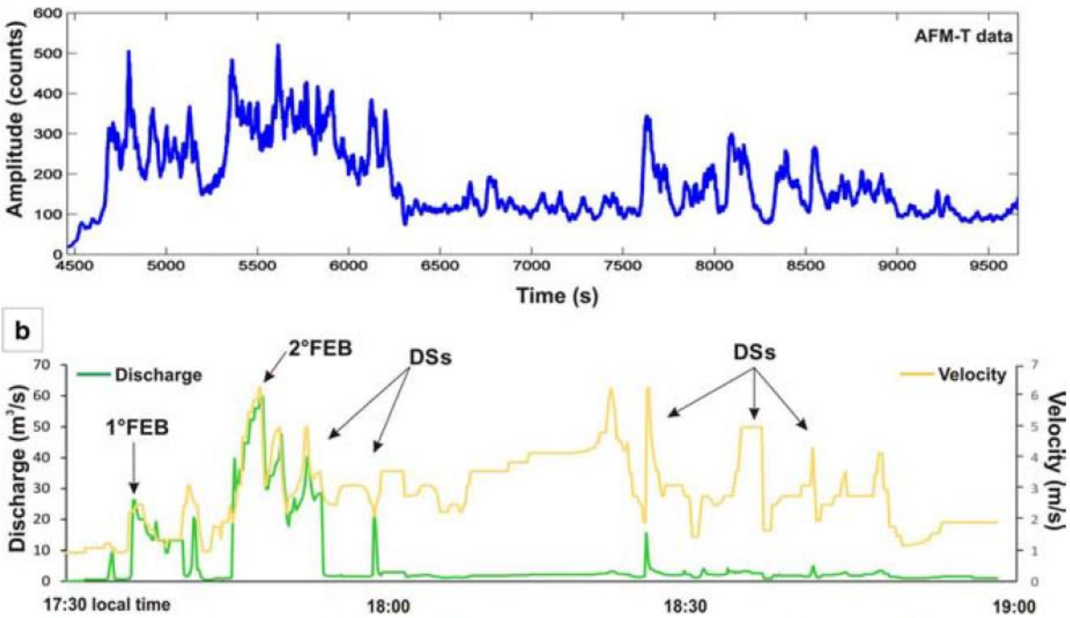

Fig. 5 Plots of the data recorded during the 11 June 2013 lahar from 17:30 to 19:00 (local time). a Envelope of the AFM-T signal (the seismic amplitude is in counts). b Comparative plot where the *green line* describes the discharge curve in m^3/s and the related values of superficial velocity in m/s (*yellow line*), both obtained from the recorded images. *Black arrows* indicate the main features of the flow, as observed in Fig. 4

To better state this concept we slightly change the text at line # 183.

In particular, for lahars at Volcán de Colima a correlation between the maximum peaks in amplitude and the maximum peaks in flow discharge was found (Fig. 5 in Vázquez et al., 2016). Fluctuation in seismic energy along the vertical component reflects variation in flow discharge.

2 (line 37). This sentence is unclear, there appear to be some key words missing. Some kind of couple

Here we refer that based on rainfall data of Manuel and Patricia hurricanes, which show a very similar behavior, a "synthetic" rainfall curve has been designed (in accumulated percentage). If the amount of rain can be estimated prior to an event, this curve could be used to run a rainfall-runoff simulation to try to have a possible forecast. The sentence was modified as it:

*A **theoretical rainfall distribution curve** was here designed based on the rainfall/time distribution of hurricanes Manuel and Patricia. Then, weather forecasts can be used to run simulations prior to* *the actual event, in order to estimate the arrival times of main pulses, usually characterized by block-rich fronts, which are responsible for most of damage to infrastructures and loss of goods and lives.*

3(line 44). Hurricanes and cyclones are not globally distributed.

We modified the sentence as suggested:

"In recent years hurricanes have had catastrophic effects on volcanoes in the tropics troughs the triggering of lahars (sediment-water gravity-driven flows on volcanoes)."

3A(line 55). Mt Ruapehu is not a tropical volcano, despite its rich rain-triggered lahar

The Mt. Ruapehu reference was deleted.

4 and 6 (line 164 and 188). Insert the full date.

The full date for Patricia and Manuel date of landfalls were added.

In contrast, in 2015 the MgMS site was destroyed by pyroclastic flows during the 10-11 ***July*** *explosive activity, and in October 2015 the new station was still under construction.*

Hurricane Manuel (category 1), hit the Pacific coast on 15 September 2013 causing several damage to mountainous region in Guerrero state, triggering several landslides that caused up to 96 deaths and left several villages cut of, as while thousands of tourists were trapped at Acapulco and Ixtapa international airports.

6A (line 200). The sentence was modified as suggested.

Hurricane Patricia on 2015 was considered as the strongest hurricane on record to affect Mexico. The system ***began*** *to develop on 18 October over the Pacific Ocean, strengthened into a hurricane shortly after 00:00 GMT on 22 October and early on 23 October it reached its maximum category of 5,* ***before losing strength as it moved onto the Sierra Madre Occidental range****.* ***Landfalls occurred around*** *23:00 GMT on 23 October along the coast of the Mexican state of Jalisco near Playa Cuixmala, about 60 km west-northwest of Manzanillo.*

7(line 234). This sentence reads like there are three zones, unless you are combining the channel and terraces into one. Clarify please.

The sentence was clarified:
The watershed of La Lumbre and Montegrande ravines were subdivided into ***two main zones: 1)*** *the unvegetated upper cone* ***and the main channel*** *that both consist of unconsolidated pyroclastic material with large boulders embedded in a sandy to silty matrix,* ***and 2) the*** *vegetated lateral terraces.*

.
7A (line 279). Move this sentence to line 173.
This sentence was moved as suggested (se answer to point 1)

8 and 9 (line 311-329). Move the underlined text down to line 316 and move the indicated block of text to line 316 before the insertion.
Done

Finally, analyzing the simulation in the Montegrande ravine for the 11 June 2013 event, it is possible to observe a different behavior. The lahar starts as less than the 10% of the total rain is accumulated, and the main lahar pulses perfectly correlate with the peak rainfall intensities, and only the last largest pulse correlates with the watershed peak discharge. For la Lumbre watershed, in 2015 a clear correlation between peak rainfall intensities and simulated watershed discharge is not clear. For the Patricia event, along the La Lumbre ravine, first slurry flows also starts after 40% or total rainfall, but main lahar pulses fit better with the simulated peaks watershed discharge.

10. A critical weakness of using the 40% of total rainfall threshold is that it is difficult to know when this point has been reached when it is still raining, unless you have a great deal of faith in your weather forecasts. Do you have accurate predicted total rainfall and distribution curves for these events that could be run through your simulator and compared with the actual lahar events?

We agree with the reviewer. Here we are only pointing to the evidences get from data here presented (not from the simulations!) that after 40% of the total rainfall first lahars are detected for all the analyzed events. This corresponds to an amount of accumulated rainfall of 100, 120 and 160 mm of rain for Jova, Manuel and Patricia respectively. This evidence points that after at least 100 mm of rains had accumulated (measured in real time from raingauges) lahars can occur.
The early warning system will be based on rainfall-runoff modeling results. For the Patricia event the trajectory and time of landfall was quite well predicted, and data about the amount of rainfall were also provided. The text was modified as follow:

For the Jova, Manuel and Patricia events, lahars started after the 40% of total rain had accumulated ***(corresponding to c. 100, 120 and 160 mm of rain respectively),*** *and apparently the timing for the initial pulses correlates well with the peaks of the rainfall intensity for the Montegrande ravine, while for La Lumbre ravine they better match with the peak simulated watershed discharge.*

11 (line 335). This implies that there is no lag time between the peak rainfall intensity measured 6 km away on another volcanic edifice and the arrival of the lahar peak at the detectors.

As observed for the Hurricane Jova, rainfall data from the station at Montegrande and La Lumbre ravine are almost identical (more than 8 km away). This means that the rainfall behavior is quite constant over a large area during a hurricane. Similar behavior is observed for Patricia event, by comparing the Nevado station with the raingauge at Ciudad de Colima. So even if data here used for the Hurricane Patricia are from a station located 6 km away from Volcan de Colima, we are considering that the rainfall intensity was quite homogeneous over these two volcanoes. The following figure will be added as an extra panel to Fig. 3.

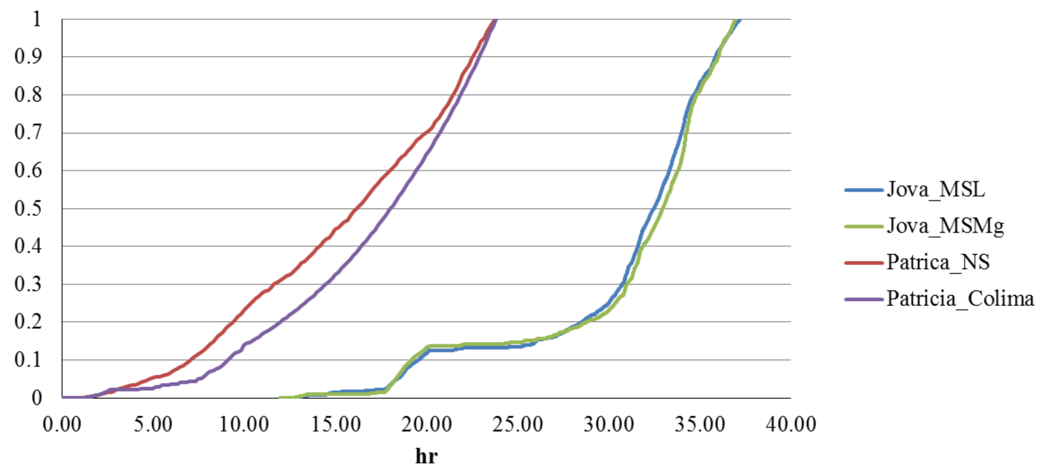

Fig. R2. Normalized rainfall of the Jova and Patricia event as gathered form different stations, pointing to a quasi-stationary rainfall behavior.

12. How long does it take to run Flo-2d, could it be run in real-time by feeding in the incoming rainfall intensity data?
For the simulation here performed, using a 20 m DEM in resolution, each simulation took no more than 30 minutes at our facility so yes, it could be possible to run simulation in real time as data are acquired.

13. Clarify.
The phrase was slightly modified

*The observed difference between Montegrande and La Lumbre ravines can be correlated with the different areas and shapes of the two catchments. In fact, due to its elongated shape (K_G = 1.7) and small area (2 km^2), the Montegrande watershed shows a quicker response between rainfall and discharge, **with a rapid water concentration** at different point along the main channel (Fig. 1b).*

14. So the simulation cannot duplicate the initial hydrophobic behaviour?

No, with the parameter here used, even changing the SCS to 95% (almost impermeable) the simulation was not able to reproduce water discharge at the time the lahars were detected. This is probably again related with the initial abstraction that is fixed by the program based on the CN value (see comment below and responses to reviewer RC2).

15. I'm assuming that these catchments are ungauged, so there is no way of calibrating the simulated discharge produced by the rainfall-runoff routing model?

Yes the reviewer is correct, direct measurement of watershed discharge is not available. Also based on the comments by the other reviewers we added a section to try to validate the simulation using the video images recorded by La Lumbre monitoring station. Apparently first stream flows are detected at the same time the simulated watershed discharge curve increases. Please refer to response to reviewer RC2 for more detail on this point.

Hydrological control of large hurricane-induced lahars: evidences from rainfall-runoff modelling~~rainfall~~, seismic and video monitoring.

Con formato: Fuente: Sin Cursiva

Lucia Capra[1], Velio Coviello[1,2], Lorenzo Borselli[3~~2~~], Víctor-Hugo Márquez-Ramírez[1], Raul Arámbula-Mendoza[~~3~~4]

[1] Centro de Geociencias, Universidad Nacional Autónoma de México (UNAM), Campus Juriquilla, Queretaro, México

[2] Free University of Bozen-Bolzano, Facoltà di Scienze e Tecnologie, Italy

[~~2~~3] Instituto de Geología, Universidad Autónoma de San Luis Potosí, San Luis Potosí, México

[~~4~~3] Centro Universitario de Estudios e Investigaciones en Vulcanología (CUEIV), Universidad de Colima, Colima, México.

Abstract

Con formato: Español (México)

The Volcán de Colima, one of the most active volcanoes in Mexico, is commonly affected by tropical rains related to hurricanes that form over the Pacific Ocean. In 201~~0~~1, 2013 and 2015~~6~~ hurricanes Jova, Manuel and Patricia, respectively~~,~~ ~~promoted~~ triggered tropical storms that ~~accumulated~~ deposited up to 400 mm of rain in 36 hrs, with maximum intensities of 50 mm/hr~~s~~. Effects were devastating, with the formation of multiple lahars along La Lumbre and Montegrande ravines, which are the most active channels in sediment delivery on the S-SW flank of the volcano. Deep erosion along the river channels and several marginal landslides ~~at their side~~ were observed, and ~~damages to bridges and paved roads for~~ the arrival of block-rich flow fronts resulted in damages to bridges and paved roads in the distal reaches of the ravines. ~~Based on data from real-time monitoring~~

~~(including images, seismic records and rainfall data), t~~The temporal sequence of these flow events is reconstructed and analyzed using monitoring data (including video images, seismic records and rainfall data) with respect to the rainfall characteristics and the hydrologic~~al~~ response of the watersheds based on rainfall-runoff~~/infiltration~~ numerical simulation. For the studied events, lahars occurred ~~after~~ 5-6 hours after the onset of~~since~~ rainfall~~ started~~, lasted several hours and were characterized by several pulses with block-rich fronts and a maximum flow discharge of 900 m^3/s. Rainfall~~/infiltration~~-runoff simulations were performer ~~with the Flo-2D code~~ using the SCS-Curve N~~n~~umber and ~~)~~ ~~infiltration model.~~ the Green-Ampt infiltration-models, providing similar result in detecting simulated maximum watershed peaks discharge.- Results show a different behavior~~s~~ for the arrival times of the first lahar pulses that correlate with the simulated catchment's peak discharge for La Lumbre ravine and with the peaks in rainfall intensity for Montegrande ravine. This different behavior is ~~strictly~~ related to the area and shape of the~~se~~ two watersheds. ~~Nerveless~~Nevertheless, in all~~for all the~~ analyzed cases, the largest- lahar pulse always corresponds with the last one and correlates with the simulated maximum peak discharge of these catchments. Data presented here ~~presented~~ show that ~~main~~ flow pulses within a lahar are not randomly distributed in time, and they can be correlated with rainfall peak intensity and/or watershed discharge, depending on the watershed area and shape. This outcome has important implications for hazard assessment during extreme hydro-meteorological events since it could help in providing real-time alerts. A ~~stormwater~~ theoretical rainfall distribution curve was ~~here~~ designed for Volcán de Colima based on the rainfall/~~-~~time distribution of hurricanes Manuel and Patricia. ~~and, in case on available weather forecasts,~~ This ~~it~~ can be used to run simulations using weather forecasts prior to the actual event, in order ~~and have an~~ to estimat~~e~~~~ion~~ ~~of~~ the arrival time~~ arrivals~~ of main lahar pulses, usually characterized by block-rich fronts, ~~that~~ which are responsible ~~of~~ for most of damage to infrastructures and loss of goods and lives.

***Keywords**: lahar, hurricane, rainfall/~~infiltration~~ runoff ~~simulation~~modeling, Volcán de Colima, Mexico.*

1. Introduction

In ~~past~~ recent years hurricanes have had catastrophic effects on volcanoes in the tropics ~~of the world~~ troughs the triggering of lahars (sediment-water gravity-driven flows on volcanoes). One of the most recent episodes is represented by the ~~2009~~ Hurricane Ida in El Salvador in 2009 that caused several landslides and debris flows from the Chichontepec volcano, killing 124 people.~~, or by the~~ In~~,~~ 1998 Hurricane Mitch ~~that~~ triggered the collapse of a small portion of the inactive Casita volcano (Nicaragua), originating a landslide that suddenly transformed into a lahar that devastated several towns and killed 2000 people (Van Wyk Vries et al., 2000; Scott et al., 2005). A similar event was observed in 2005 when tropical storm Stan triggered landslides and debris flows from the Toliman Volcano (Guatemala), causing more than 400 fatalities at Panabaj community (Sheridan et al., 2007). Other examples can be found at ~~the volcanoes~~ Pinatubo (Philippines), Merapi and Semeru (Indonesia)~~,~~ Soufriére Hills (Montserrat) and Tungurahua (Ecuador) volcanoes ~~,~~ ~~Mt. Ruapehu (New Zealand),~~ where tropical storms and heavy rainfall seasons have triggered high-frequency lahar events (Umbal and Rodolfo, 1996; ~~Cronin et al., 1997;~~ Lavigne et al., 2000; ~~-~~Lavigne and Thouret, 2002; Barclay et al., 2007; Dumaisnil et al., 2010; Doyle et al., 2010, de Bélizal et al., 2013 Jones et al., 2015).

Volcán de Colima (19°31’N, 103°37’ W, 3860 m a.s.l., Fig. 1), one of the most active volcanoes in Mexico, is periodically exposed to intense seasonal rainfalls that are responsible for the occurrence of lahars from June to late October~~ (Davila et al., 2007; Capra et al., 2010).~~ ~~Rain-triggered lahars represent a very common process during the rainy season (June-October) at Volcán de Colima~~ (Davila et al., 2007; Capra et al., 2010; Vá~~a~~zquez et al., 2016a). ~~They~~ Lahars usually affect areas as much as 15 km from the summit of the volcano, with resulting damage to bridges and electric power towers (Capra et al., 2010), and are more frequent just after eruptive episodes such as dome collapses ~~emplacing~~ that emplace block-and-ash flow deposits (Davila et al., 2007; Vázquez et al., 2016b). Several hurricanes commonly hit the Pacific Coast each year and proceed inland as tropical rainstorms reaching the Volcán de Colima area. In particular~~,~~ ~~on~~ in 2011, 2013 and 2015 Hurricanes Jova, Manuel and Patricia ~~hurricane~~ respectively triggered long-lasting lahars along main ravines draining the edifice, causing sever~~eal~~ damages ~~on~~ to roads and bridges, and leaving ~~leaven uncommunicated for few days several~~ communities in a radius of 15 km from the volcano cut off for several days~~.~~

Previous work (Davila et al., 2007; Capra et al., 2010) analyzed ~~the~~ lahars frequency at Volcán de Colima in relation ~~with the~~to eruptive activity and ~~the~~ rainfall characteristics ~~of rainfalls~~. Lahars are more frequent at the beginning of the rainy~~s~~ season, during short (< 1 hour) no-stationary rainfall events~~s~~, with variable rainfall intensities and with only 10 mm of accumulated rainfall. This behavior has been attributed to a hydrophobic effect of soils on the volcano slope (Capra et al., 2010). In contrast, in the late rainy season, when tropical rainstorms are common, lahars are triggered depending on the 3-day antecedent rainfall and with intensities that increase as the total rainfall amount increases (Capra et al., 2010). The

Con formato: Inglés (Estados Unidos) lahar~~s~~ ~~record~~ catalog used for these previous studies was based only ~~based~~ on seismic data. Since 2011 a visual monitoring system ~~have~~ has been installed on the Montegrande and La Lumbre ravines (Figure 1), based on which a quantitative characterization of some events (i.e type of flow, velocity, flow discharge, flow fluctuation) have been possible (i.e. Vázquez et al., 2016a; Coviello et al., under revision). The aim of the present paper is to better understand the ~~lahars~~ initiation processes of large lahars and their dynamic~~al~~ behavior, especially during hurricane events, when more damage~~s~~ ~~have~~ has been observed on inhabited areas. In particular, the arrival time of the main lahar's front/surge at the monitoring stations is ~~here~~ analyzed with respect to ~~the~~ rainfall characteristics (rain accumulation and intensity) and in relation ~~with~~ to the watershed's hydrological response ~~of the watersheds~~ based on a rainfall/~~infiltration~~ runoff numerical simulation.

The occurrence of discrete surges within debris flows and lahars ~~have~~ has been attributed to spatially and temporally distributed ~~lahar~~ sediment sources, temporary damming, progressive entrainment of bed material or change in slope angle (~~i.e.~~ Iverson 1997; Marchi et al. 2002; Takahashi 2007; Zanuttigh and Lamberti 2007; Doyle et al., 2010; Kean et al., 2013). Without excluding previous models, data from large lahars triggered by Hurricanes Jova, Manuel and Patricia ~~here presented~~ show~~s~~ that main pulses within a lahar are not randomly distributed in time, and they can be correlated with rainfall peak intensity and/or watershed discharge, depending on: 1) ~~the~~ watershed shape, and 2) hydrophobic behavior subject to the antecedent soil moisture. These lahars ~~triggered by the hurricanes Jova, Manuel and Patricia are here used as they correspond with the best documented events occurred during past years, and they~~ are~~will be~~ also compared with a flow triggered by an extraordinary hydrometeorological event that occurred at the begin of the rain season (11

June, 2013) to better show the drastic change on lahar initiation due to the hydrophobic effect of soils at Volcán de Colima. Based on rainfall distribution over time for the analyzed events, a ~~stormwater~~ theoretical rainfall distribution curve is here designed, which can be used to run simulations prior to an event to have an estimation of the time arrivals of main pulses when weather forecast is available. ~~The data~~Results here presented have important implication for hazard assessment during extreme hydrometeorological events and can be used as a complementary tool ~~of~~ to develop an ~~an e~~Early ~~w~~Warning ~~s~~System (EWS) for lahars on tropical volcanoes. ~~.~~

2. **Methods and data**

2.1. La Lumbre and Montegrande watersheds

The source area of rain-triggered lahars at Volcán de Colima corresponds to the uppermost unvegetated portion of the cone (Fig. 1 and 2a), with slopes between 35° and 20°, that also corresponds with an area of high connectivity, being prone to rill~~s~~ formation and erosive processes (Ortiz-Rodriguez et al., 2017). The channels along main ravines have slopes that vary from 15° proximally up to a maximum of 4° in the more distal reaches. ~~,~~ T~~t~~hey are flanked by densely vegetated terraces, up to 15 m high ~~in~~ average, that consist of debris avalanche and pyroclastic deposits from past eruptions (Figs. 2b and c) (Cortes et al., 2010; Roverato et al., 2011). Seven major watersheds ~~from 2 to 14 km^2~~ feed the main ravines draining from the volcano on the southern side (Fig. 1). La Lumbre is the largest watershed, with a total area of 14 km^2, and Montegrande is ~~in average~~representative ~~with~~ of the other catchments~~,~~ with an area of 2 km^2 (Fig. 1). Beside the difference in total area, the

Montegrande and La Lumbre watersheds are quite different in geometry. Montegrande catchment is elongated, with a maximum width of 800 m~~,~~ (300 m ~~in~~ average). In contrast, the proximal portion of ~~the~~ La Lumbre catchment includes ~~all~~ the entire~~the~~ NW slope of the cone, before elongating ~~to then extent to a more elongated shape~~ towards the SW, being up to 1500 m in width. These differences in area and shape can be correlated with a different water discharge response ~~in water discharge under a~~during a rainfall event. In circular drainages, ~~as~~ i.e. the proximal portion of ~~the~~ La Lumbre watershed, all points are ~~quite~~ equidistant from the main ~~river~~ channel so all the precipitation reaches the river at the same time, concentrating a large volume of water. In contrast, in a more elongate basin, lateral drainages quickly drain water into~~on~~ the main channel at different points ~~but~~ resulting in ~~with~~ a lower total discharge. The Gravelius's index Kg (Gravelius, 1914; Bendjoudi and Hubert 2002), which is defined as the relation between the perimeter of the watershed (P) and that of a circle having a surface equal to that of a watershed (A):

$$Kg = \frac{P}{2\sqrt{\pi A}}$$

is here estimated for Montegrande watershed and for the upper, circular portion of La Lumbre watershed, obtaining values of 1.7 and 1.1 respectively. The lower the value, the more regular the basin's perimeter and the more prone it is to present high runoff peaks. Based on these considerations, at La Lumbre watershed a larger volume of water concentrates along the main channel because of its larger surface and circular shape, but after a larger period of time ~~respect~~ relative to the Montegrande ravine, where a minor volume of water quickly reaches the main drainage.

2.2 Lahar Monitoring at Volcán de Colima

In 2007, a monitoring program was implemented at Volcán de Colima. ~~At the beginning~~Initially, two rain gauges w~~h~~ere installed to study lahar initiation (AR and PH sites, Figure 1) and lahar propagation was detected ~~by~~ using the broadband seismic stations of RESCO, the seismological network of Colima University (Davila et al., 2007; Zobin et al., 2009; Capra et al., 2010).~~ Afterwards, t~~Two monitoring station specifically designed for studying lahar activity were installed later, in 2011 at the Montegrande ravine and in 201~~4~~3 at La Lumbre ravine (MSMg and MSL respectively, Figure 1). Both stations consist of a 12 m-high tower with a directional antenna transmitting data in real time to RESCO facilities, a camcorder recording images each 2-4 secs with a 704 x 480 pixel~~s~~ in resolution, a rain gauge coupled with a soil moisture sensor, and a 10 Hz geophone (Vázquez et al., 2016a; Coviello et al., under revision). The rain gauge (HOBO RG3) records rain accumulation at one-minute intervals. At Montegrande ravine seismic data are also obtained from a 3 component Guralp CMG-6TD broadband seismometer installed ~~at~~ 500 m upstream from the monitoring site, sampling at 100 Hz (BB-RESCO, Figure 1).

The Montegrande station detected lahars ~~occurred~~ during the 2011 Jova and 2013 Manuel events, ~~and~~ while lahars triggered during ~~the 2015 Hurrican~~Hurricane Patricia in 2015 were only recorded by La Lumbre station (Table 1). ~~In fact, in~~In 2011, only the ~~Mg~~MSMg site was ~~operating~~ operational (as the BB-RESCO station), and recorded the seismic signal of ~~the~~ lahars associated ~~to~~ with Jova and Manuel events. No images are available since both events occurred during the night. The ~~L~~MSL station ~~starts~~ began to operate at the end of 2013 and was able to record ~~the~~ lahars associated ~~to~~ with Hurricane Patricia along the La Lumbre ravine (images and geophone data). In contrast, in 2015 the ~~Mg~~MSMg site was destroyed by pyroclastic flows during the 10-11 July explosive activity, and in October 2015 the new station (MSMg_2015) was still under construction. Only a few pictures were acquired and they are of low quality because of the abundant steam coming from thegenerated by hot lahars since they originated from the remobilization of fresh pyroclastic flow deposits (Capra et al., 2016). The 11 June 2013 event was perfectly captured by the camera installed at the MgMSMg site and the BB-RESCO recorded its seismic signal.

The seismic signal is here analyzed to detect the arrival of main flow fronts and to estimate the discharge variation. For this, only the amplitude of the signal is considered, which can be correlated with the variation in the maximum peak flow discharge (Doyle et al., 2010; Vázquez et al., 2016a). In particular, for lahars at Volcán de Colima a correlation between the maximum peaks in amplitude and the maximum peak in flow discharge was found (Fig. 5 in Vázquez et al., 2016a). Fluctuation in seismic energy along the vertical component reflects variation in flow discharge.

The seismic record is here compared with the available images to identify the main changes in lahar dynamics of the detected lahars. All the lahars here analyzed correspond to multi-pulses events as classified by Vááazquez et al. (2016a); they consist of long lasting lahars presenting several pulses, each one characterized by a block-rich front followed by the main body and dilute tail showing continuous changes in flow discharges. A detailed seismic description of these types of lahar typess at Volcán de Colima is available in Vázquez et al. (2016a);:, here we focus on the number of main flow peaks and their arrival times.. (Table 2).

2.3. The hydrometeorological events

Hurricane Jova formed over the Pacific Ocean, hit the Pacific coast on October 12, 2011, as a category 2 event, and traveled inland toward Volcán de Colima. The hurricane arrived as a tropical storm at the town of Coquimatlán, just 10 km SW of the city of Colima with winds of up to 140 km/hr, and 240 mm of rain ~~over~~ falling over 24 hrs (Fig. 3a). Severe damage was registered in inhabited areas, including the city of Colima where floods damaged roads, bridges and buildings.

~~The 2013~~ Hurricane Manuel ~~of~~ (category 1), hit the P~~p~~acific coast on 15 September 2013 ~~during national holidays (Fiestas Patria)~~ causing several damage to mountainous region in Guerrero state, triggering several landslides that caused up to 96 deaths and left several villages ~~uncommunicated~~ cut of, ~~as~~ while thousands of tourists were trapped at Acapulco and Ixtapa international airports. At Volc~~a~~án ~~the~~ de Colima rain~~s~~ started on September 15 and lasted for more than 30 hrs with more than 300 mm of ~~accumulated rains~~falling (Fig. 3a).

~~The 2015~~ Hurricane Patricia on 2015 was considered as the strongest hurricane on record to affect Mexico. The system ~~starts~~ began to develop on 18 October over the Pacific Ocean, strengthened into a hurricane shortly after 00:00 GMT on 22 ~~-~~October and early on 23 October it reached its maximum category of 5, before losing strength as it moved onto the Sierra Madre Occidental range~~. But late on the same day, the system rapidly lost its strength~~. ~~It l~~Landfalls occurred around 23:00 GMT on 22~~3~~ October ~~a~~along the coast of the Mexican state of Jalisco near Playa Cuixmala, about 60 km west-northwest of Manzanillo. On the morning of the 23 October, 2015 it continued to rapidly weaken~~ as it moves on the~~

~~Sierra Madre Occidental high relieves~~. At Colima town, up to 400 mm of rains ~~accumulated~~ fall ~~along~~ on 30 hours ~~since~~ after the morning of 23 October (Fig. 3a). Lahars along the Montegrande ravine were hot since they originated from the erosion of pyroclastic flow deposits emplaced during the 10-11 July 2015 eruption. Severe damages affected ~~the~~ Colima town and areas ~~the volcano~~ surrounding the volcano. A bridge along the interstate was destroyed ~~leaving uncommunicated~~ cutting of La Becerre~~a~~ra village and interrupting ~~the~~ traffic between Colima and Jalisco states.

2.3.1 Rainfall during hurricanes

Rainfall data were obtained from different rain gauge stations (Table 1 and Fig. 1). In particular, for the events studied at Montegrande ravine, rainfall data came from the rain gauge installed at SMMg while for the Patricia event, the more proximal available rain station is located at the top of the Nevado de Colima volcano (NS, Fig 1). It is worth mentioning that at Volcán de Colima, during stationary rainfall events associated to hurricane, no important differences in rainfall duration and intensity are detected at regional scale. For instance, the measured rainfall associated to Hurricane Jova was alike at two rain gauges located at more than 7 km of distance (MSMg and MSL) and during Hurricane Patricia same duration and intensity values were recorded by station NS and a station located in the Colima town, 30 km S from the volcano summit (Fig. 3b~~a~~). Patricia and Manuel rainfalls show ~~a~~ similar behavior, with ~~a~~ progressive rain accumulation ~~along~~ over 28-30 hrs; in contrast, during Hurricane Jova, 200 mm of rain ~~accumulated~~ fell in less than 15 hrs, with only another 40 mm ~~reaching a total of 240 mm during the~~ falling during the following 13 hrs (Fig. 3~~b~~a~~a~~). These differences are more evident plotting the 10-min accumulated value normalized over the total accumulated rainfall (Fig. 3c~~b~~). Average rainfall intensities calculated over a 10-min interval range from 32 mm/hr~~s~~ to 37 mm/hr~~s~~ for Manuel and Patricia events respectively and up to 43 mm /hr~~s~~ for the Hurricane Jova (Table 1~~2~~). Finally rainfall values were calculated at selected time intervals (~~15~~ 0.25~~m~~, ~~30~~ 0.5~~m~~, ~~45~~ 0.75~~mm~~, 1, 3, 6, 12, 18, 24, 2~~8~~7 hr~~r~~) to design possible storm rainfall distributions based on tropical rains associated ~~t~~with~~o~~ hurricanes recorded historically ~~so far~~ at Volcán de Colima ~~Volcano~~ (Table 2). Considering the similar behavior of the Manuel and Patricia rainfalls, a theoretical rainfall distribution curve ~~a stormwater~~ can be designed considering their average values (Fig. 3d~~e~~) (i.e. NRCS, 2008), based on which a forecast analysis can be performed, as will be discussed below.

2.4. ~~Rainfall~~ Rainfall-runoff modelling~~simulations~~

To better understand the lahar behavior and duration during extreme hydrometeorological events at Volcán de Colima, ~~rainfall~~ rainfall-runoff simulations ~~simulations~~ were performed with Flo-2D code (O´Brie~~a~~n et al., 1993). The Flo-2D code routes the overland flow as discretized shallow sheet flow using the Green-Ampt or the SCS Curve number (or combined) infiltration models. For the present work the SCS Curve Number (SCS-CN, i.e. Mishra and Singh, 2003) was selected for the analysis and a comparison between both infiltration models is presented below. The rainfall is applied to the entire watershed, without spatial variability because we are dealing with large-scale, long duration hurricane-induced rainfall. This rainfall is discretized as a cumulative percent of the total precipitation each 10 minutes. With the SCS-CN~~is~~ model, the volume of water runoff produced for the simulated precipitation is estimated through a single parameter, i.e. the Curve Number

Con formato: Espacio Después: 0 pto

(CN). This parameter ~~that~~ summarizes the influence of both the superficial aspects and deep soil features, including the saturated hydraulic conductivity, type of land use, and humidity before the precipitation event (for an accurate description of the origin of the method see Rallison, 1980; Ponce and Hawkins, 1996). A similar approach was ~~already~~ previously used for modeling debris flow initiation mechanisms (i.e. Gentile et al., 2006; Llanes et al., 2015). To apply the SCS-CN model, it is necessary to classify the soil in one of four groups, each identifying a different potential runoff generation (A, B, C, D; USDA-NRCS 2007). The watershed of~~-~~ La Lumbre and Montegrande ravines were subdivided into two main zones: 1) the unvegetated upper cone and the main channel that consists of unconsolidated pyroclastic material with large boulders e~~i~~mbedded in a sandy to silty matrix, and 2) the vegetated lateral terraces. Lateral terraces consist of old pyroclastic sequences~~,~~ with incipient soils and are vegetated with pine trees and sparse b~~r~~ushes~~,~~. ~~with soils that show a hydrophobic behavior at the beginning of the rain season (Capra et al., 2010). In situ infiltration tests were also performed based on which values of saturated conductivity were obtained in the range of 50 mm/h (nude soil) to 100 mm/h (vegetated) (Ortiz, 2017).~~ Based on these observations, soils were classified between group A and B (Bartolini and Borselli, 2009). ~~Curve Numbers~~ CN values for the vegetated terraces and for the nude soils were estimated ~~in~~ at 75 and 80 respectively (in wet season, Hawkins et al., 1985; Ferrer-Julia et al. 2003). To ~~perform~~ perform a simulation with the FLO-2D code, two polygons were traced to delimit the un-vegetated portion of the cone from the vegetated area of the watershed, and at each polygon the relative CN value was assigned. ~~The simulated rain corresponds with the cumulative value calculated at 10 minutes interval (Fig. 3b).~~ At the apex of each watershed a barrier of outflow points were defined to obtain the ~~total~~ values of the simulated watershed discharge computed at each 0.1 hr. The simulation was performed with a 20-m digital elevation model. One of the limitations of the SCS method is that it does not consider the effect of the rainfall intensity on the infiltration. In addition, since no measurements of water discharge are available at both La Lumbre and Montegrande basins, it is difficult to calibrate the simulations here presented. To investigate the SCS-CN model uncertainties, the Green-Ampt (1911) model (G-A), sensitive to the rainfall intensity, was also applied and the results were compared with the outcome of the SCS-CN model. For the G-A method, the main input parameters are the saturated hydraulic conductivity (Ks), the soil suction and volumetric moisture deficiency. The Ks is a key factor in the estimation of infiltration rates and exerts a notable influence on runoff calculations, therefore requiring great care in its measurement (Grimaldi et al., 2013). The input values can be extrapolated from tables or directly measured with field experiments. Based on the textural characteristics of soils and type of vegetation at Volcán de Colima, input parameters were selected based on available tables in the Flo-2d PRO reference manual (Table 3). In particular, with a Ks value of 20 mm/hr the simulated watershed discharge best fits with the precursory shallow-water flow observed in the images, as it will be showed below (Figure 4). The Ks value of 20 mm/hr is equivalent to the CN value used for the SCS-NC simulations. In fact an empirical relation between Ks and CN has been proposed be Chong and Teng (1986):

$$S = 3.579Ks^{1.208}$$

where S is the potential retention related to the CN as follow (Mockus, 1972):

$$CN = \frac{2540}{S + 25.4}$$

Based on these equations a value of Ks equal to 20 mm/hr corresponds to a CN of 75.5 in the range of values here used for the SCS-NC infiltration model.

The G-A infiltration model was tested in La Lumbre ravine, using the Patricia event and comparing the simulated watershed discharge curve with the available video images. Figure 4 shows the discharge curve that best fits the data gathered from the images, based on which the two methods were qualitatively calibrated. The G-A infiltration method nicely reproduce the initial scouring of a muddy water corresponding with the first increase in the simulated watershed discharge. The SCS-CN infiltration model is not able to reproduce this first water runoff. This can be explained considering that the initial abstraction due to the interception, infiltration and surface storage, is automatically computed in the SCS-NC method as 0.2S, being probably too high for the studied area. In contrast, with the G-A method, the initial abstraction can be modified and best results were obtained with a value of 6 mm corresponding to a surface typical of a vegetated mountain region. However, both infiltration models give similar results for the main peaks of the simulated maximum watershed discharge that correspond to the arrival of the main lahar pulses observed in the images (Fig. 4). These results show that the G-A model is much more reliable to detect precursory slurry flows, while both models are equally able to catch the main surges of a lahar. One important point is that the simulations are here used to set up an EWS to forecast the lag time of the main lahar surges. The first slurry flows were important to calibrate the G-A simulation but they do not represent an essential data for the EWS. In addition, input data for the G-A method often are difficult to set, requiring great care in its measurement; in contrast, the output of the SCS-CN method only depend from the CN value. The SCS-CN method has been largely used in rainfall-runoff modeling, and we consider that it is a valuable method for the objective of the present work, as we are not seeking a quantitative estimation of the watershed discharge but the arrival times of the main lahar pulsesd.

A sensitive analysis of the G-A input parameters presented in previous works (i.e. Chen et al., 2015) shows that the saturated hydraulic conductivity Ks is a key factor in the estimation of infiltration rates and exerts a notable influence on runoff calculations (i.e. Chen et al., 2015). With respect to the SCS-CN model, the only input parameter is the CN, thus we present a simple comparison for the Patricia event at La Lumbre ravine. Results obtained with the 80/75 CN values for channel and vegetated area respectively, are compared to two other simulations performed using global values of 75 and 80 (see tTable 43). This exercise shows that the uncertainty in simulated maximum peak discharge is in the range of 0.1 hr, pointing that a global CN value could also be used for the Volcán de Colima.

Con formato: Sin Resaltar

Con formato: Sin Resaltar

Con formato: Sin Resaltar

Con formato: Sin Resaltar

Con formato: Sin Resaltar

Con formato: Sin Resaltar

Con formato: Sin Resaltar

Con formato: Sin Resaltar

3. Results

During the Hurricane Jova hurricane, lahars started at around 07:20 GMT (all times here after reported as GMT) in the Montegrande ravine early in the morning of 12 October, 2011, around 07:20 GMT (here after all time is in GMT), after approximately c. 40 % of the total rain (240 mm) accumulated had fallen (Fig. 54a). The event lasted more than 4 hours, and three main peaks in amplitude can be detected in the seismic signal (Fig. 54a). In particular, Tthe first two peaks are similar in amplitude (0.015 cm/s) and, separated by more than 2 hours of signal fluctuation. After lLess than one hour after from the second peak, a single, discrete pulse can be recognized (0.05 cm/s in amplitude), followed by a "train" of low-amplitude seismic peaks that lasted for more than an hour.

Along the same ravine, an extreme event was recorded on 11 June, 2013. This event corresponds to an extraordinary episode and is here introduced to better discuss the hydrological response of the Montegrande ravine. It represents an unusual event at the beginning of the rainy season, considering the total accumulated rainfall ofwith 120 mm of rain falling in less than 3 hrs (Table 2), withand a maximum peaick intensity of up to 140 mm/hr (Fig. 54b). Based on the seismic record and the still images of the event, this lahar was previously characterized as a multi-pulse flow, with three main blocks-rich fronts (I, II and IV, Fig. 54c), with similar amplitudes (0.015-0.025 cm/s), followed by a main flow body consisting of a homogenous mixture of water and sediments (with a sediment concentration at the transition between a debris flow and an hyperconcentrated flow) (III, Fig. 54c) (Váazquez et al. 2016a). The last, more energetic pulse (0.042 cm/s) was accompanied by a water-rich frontal surge that was able to reach the lens of the camera (IV, Fig. 54c). Comparing the Jova and the 2013 eventFor both Jova and 11 June 2013 events, seismic records it is possible to note that in both events, the largest pulse corresponds with the last one. -Flow discharge was estimated for the 11 June 2013 event, with a maximum value of 120 m^3/s value for the largest pulses (IV, Figure 54b) (Váazquez et al., 2016a). For the Jova event, the only visual data available are the images of the channel the day before and the day after the event, where a deep erosion of the channel is visible (Fig. 65)., but cComparing its seismic signal with the 11 June 2013 lahar, and based on the classification criterion established for lahars at Volcán de Colima (Váazquez et al., 2016a) each main peak is inferred to corresponds to the arrival of a flow surges or to block-rich fronts followed by the body of the flow. Fluctuation in seismic energy along the vertical component reflects variation in flow discharge.

The lahar recorded during the Hurricane Manuel along the Montegrande ravine shows a similar behavior as to that described for the Jova event (Fig. 76). As it the event occurred during the night no images are available. Based on the seismic record from the BB-RESCO, lahars started around at c. 03:00, and lasted for seven hours. The event was characterized by five main pulses, which whose amplitude increases with time (0.012-0.025 cm/s), being with the last being one the largestr in magnitude (0.04 cm/s). Based on the amplitude values, the first two peaks correspond to precursory dilute flow waves followed by the three main pulses with block-rich fronts (I, II and III, Fig 76).

In the case of For the Hurricane Patricia, seismic data (from the geophone) and still images were recorded at the La Lumbre monitoring station. Based on these data, at approximately c. 16:2521:22 a slurry flows is startsdetected on the main channel (Fig. 47a). First pulses of hyperconcentrated flows were detected around 01:30 (24 October) which progressively increased in flow discharge and sediment concentration. The initial water flow rapidly evolves in a hyperconcentrated flow (Coviello et al., under revision) and Several several Several front waves were observed during flooding (I and II, Fig. 87b) for which an average flow discharge of 80-100 m^3/sec was estimated, and two main pulses arrived at 2304:30 and 0005:00 (24 October), with 6 m-depth block-rich fronts and maximum flow discharges of 900 m^3/sec (III, IV, V and VI, Fig. 87b). At around 0500:40 the seismic record detected the arrival of a third pulse. Although no images were available, the amplitude of the last pulse (0.07 cm/s) suggests it was larger than those previously described. As observed for the three previous events recorded at Montegrande ravine, the largest pulse again corresponded ~~again with~~ to the last one.

The resultss of ~~rainfall simulations~~ the rainfall-runoff simulation ~~are~~ are plotted as a normalized curve of the total runoff hydrograph (watershed discharge)~~discharge~~, along with the normalized accumulated rainfall and its intensity (calculated over a 10-min interval) (Fig. 9~~8~~). In the same plot, the arrival time of the main lahar pulses here analyzed is also indicated (red triangles, Fig. ~~8~~9). By comparing the simulated watershed discharge with rainfall intensity, a general correlation can be observed for the Montegrande basin during hurricanes Jova and Manuel ~~hurricane~~(Fig. 9a and b), contrasting with the 11 June 2013 event (Fig. 9c), where the simulation is not able to reproduce watershed discharge during the first minutes of the event when most of rainfall is accumulated and maximum rainfall intensities are detected.

~~For la Lumbre watershed a clear correlation between peak intensities and watershed discharge is not clearly observable.~~ If the arrival times of the main lahar~~s'~~ pulses are considered, the events associated to the hurricanes Jova and Manuel along the Montegrande ravine show a similar behavior. In both cases, early slurry flows are detected after ~40% of the total rain is accumulated. The main flow pulses better correlate with the highest rain intensity values, which also correspond with maximum peaks in simulated watershed discharge; the last, largest pulse corresponds with the maximum simulated peak discharge of the watershed. Finally, analyzing the simulation in the Montegrande ravine for the 11 June 2013 event, it is possible to observe a different behavior. The lahar starts as less than the 10% of rain is accumulated, ~~and~~ the main lahar pulses perfectly correlate with the peak rainfall intensities, and only the last largest pulse correlates with the watershed peak discharge.

~~-~~For L~~l~~a Lumbre watershed in 2015 a clear correlation between peak rainfall intensities and simulated watershed discharge is not clear. ~~ly observable. In contrast, f~~ For the Patricia event, along the La Lumbre ravine, first slurry flows (pulse I, fig. 7b) also starts after 40% of~~r~~ total rainfall ~~accumulated~~, but main lahar pulses fit better with the simulated peaks watershed discharge Fig. 9d). ~~Finally, analyzing the simulation in the Montegrande ravine for the June 2013 event, it is possible to observe a different behavior. The lahar starts as less than the 10% of rain is accumulated, and the main lahar pulses perfectly correlate with the peak rainfall intensities, and only the last largest pulse correlates with the watershed peak discharge.~~

4. Discussion

~~At present, several~~Various attempts have been made to define lahar initiation rainfall thresholds ~~have been already carried out for~~at different volcanoes (i.e. Lavigne et al., 2000; van Westen and Daag, 2005 Barclay et al., 2007; Jones et al., 2015; Jones et al., 2017), including Volcán de Colima (Capra et al., 2010). This study focused on ~~is mostly addressed to~~ better prediction of ~~the~~ lahar evolution during extraordinary hydrometeorological events such as hurricanes, a common long-duration and large-scale rainfall phenomenon ~~at~~ in tropical latitudes. In particular, we are interested in predicting the arrival of block-rich flow fronts that have caused severe~~al~~ damage~~s~~ during past events. Based on the seismic and visual data gathered from the events ~~here~~ analyzed here, it is possible to identify ~~evidence~~

~~which are the~~the key factors in controlling the arrival timing of main lahar~~s~~ fronts. For the Jova, Manuel and Patricia events, lahars started after the 40% of total rain had accumulated (corresponding to c. 100, 120 and 160 mm of rain respectively), and apparently the timing for the ~~initial~~ main pulses correlates well with the peaks of the rainfall intensity for the Montegrande ravine, while for L~~l~~a Lumbre ravine they better match with the peaks of the simulated watershed discharge. ~~Nevertheless for all analyzed cases, the largest pulses correspond with the last ones and correlate with the peak watershed discharge for all the analyzed examples.~~ The observed differences between Montegrande and La Lumbre ravines can be correlated with the different areas and shapes of the two catchments. In fact, due to its elongated shape (K_G = 1.7) and small area (~~A =~~ 2 km^2), the Montegrande watershed shows a quicker response between rainfall and discharge, with a rapid water ~~runoff that~~concentration ~~concentrated~~ at different point along the main channel (Fig. 1b). This behavior is much clearer for the 11 June 2013 event, which occurred at the beginning of the rain season when soils on the lateral terraces of the ravines show ~~a~~ hydrophobic behavior (Capra et al., 2010). The simulation was~~is~~ not able to reproduce any watershed discharge at the beginning of the event, because the hydrophobic behavior of the soils inhibits the infiltration and the water runoff quickly promotes lahar initiation. During this event, the first lahar pulses perfectly match with the rainfall peak intensities (except for the last major pulse), starting from the very beginning of the rainfall event. In contrast, La Lumbre ravine has a wider, rounded upper watershed (K_G = 1.1; A = 14 km^2) that is able to concentrate~~d~~ a larger volume of water ~~before to turn SW in~~entering the main channel where lateral contributions ~~can~~ still increase water discharge further. Even if ~~rainfalls~~ rain during ~~of~~ hurricanes Manuel and Patricia showed a similar behavior (Fig. 3), the catchment response of La Lumbre is clearly different with a pulsating behavior of lahars mainly

Con formato: Superíndice

controlled by the watershed discharge. Nevertheless, for all the events here analyzed, the largest pulse corresponds with the last one recorded and it correlates with the maximum simulated watershed discharge, pointing to a strong control of the catchments recharge in generating the largest and more destructive pulses. Previous works correlated the occurrence of surges within a lahar to multiple sources, such as lateral tributaries along the main channel (i.e. Doyle et al., 2010) or due to the failure of temporary dams of large clasts ~~in correspondence~~triggered by of an increase in rainfall intensity (Kean et al., 2013). Lateral tributaries are absent in both the Montegrande and La Lumbre channels and, even if an accumulation of clasts ~~it is~~were ~~-~~possible, no significant discontinuities of the channel bed can be observed upstream of the monitoring sites. Based on data presented here ~~presented~~, formation of pulses within a lahar is mostly controlled ~~with~~ by the watershed shape ~~the increase in water runoff that at a critical discharge rate mobilize a large volume of sediment where large clasts accumulate at its front. This is a well-documented mechanism (i.e. Iverson, 1997), but based on the model here proposed, the discharge rate is controlled by the watershed discharge~~ that regulates the timing ~~on~~ of the arrival of main pulses, depending on the rainfall behavior~~ and the watershed shape~~. Nevertheless, the last pulse ~~always~~ is always the largest in volume.

This model is strictly related to ~~to migratory,~~ long-duration and large-scale rainfall events hitting tropical volcanoes such as the Volcán de Colima. ~~In fact~~In contrast, during mesoscale non-stationary rainfalls, typical at the beginning of the rainy season, lahars are usually triggered at low accumulated rainfall values and controlled by rainfall intensity due to the hydrophobic behavior of soils, and they usually consist of ~~uni~~single-pulse events with~~ a~~ ~~single~~ one block-rich front that last less than one hour (i.e. Vázquez et al., 2016b). In perspective, the results presented here ~~presented~~ can be used to design an ~~Early Warning System (~~EWS~~)~~ for hurricane-induced lahars, i.e. event triggered by long-duration and large-scale rainfalls. Most common pre-event or advance-EWSs for debris flows are based on empirical correlations between rainfall and debris flow occurrence (e.g., Keefer et al., 1987; Aleotti, 2004; Baum and Godt, 2009; Jones et al., 2017; Wei et al., this volume; Greco and Pagano, this volume). The instruments adopted for debris-flow advance warning are those normally used for hydrometeorological monitoring and consist of telemetry networks of rain gauges and/or weather radar. The typical way to represent these relations is identifying critical rainfall thresholds for debris flow occurrence. The availability of both a large catalogue of events and a reliable precipitation forecast that could give the predicted amount of rainfall some hours in advance would allow the issue of an effective warning, at least in predicting the likely arrival time of the main lahar pulses. In addition, instrumental monitoring of in-channel processes can be used to validate a preliminary warning-condition triggered by ~~wheatear~~weather forecast and/or rainfall measurements.

5. Conclusions

~~Real time~~ M~~m~~onitoring data from long-lasting lahars triggered by Hurricane Jova, Mauenl and Patricia at~~of lahars at~~ Volcán de Colima ~~volcanoes reveal~~ demonstrated that watershed discharge is the key factor in controlling the arrival time of main block-rich fronts~~ during long lasting lahar triggered during tropical storms~~, and that the largest destructive pulses will arrive after the initial surges~~ing.~~ In particular, ~~F~~for the 2015 Hurricane Patricia ~~event~~ the weather forecast predicted a~~n estimated~~ value ~~for~~ of~~the~~ total rainfall, ~~as~~ and also the approximate time of its landfall the day before the event. Based on the deign~~ed~~ storm obtained with the ~~time~~ rainfall/time ~~-~~distribution of the event analyzed here~~-analyzed~~, it ~~could~~ would have been possible to anticipate when lahars started along the La Lumbre ravine, and the arrival time of main pulses. This first rough prediction of the arrival times of main lahar pulses could have been validated and updated based on real time data acquisition and rainfall-runoff simulations that do not take more than 30 minutes to provide results. ~~Along the other ravines, that show a watershed similar to the Montegrande, it could have been possible to predict the arrival of at least the largest pulse.~~ This information coupled with the real time monitoring ~~could~~ can be a ~~better~~ valuable tool to employ for hazard assessment and risk mitigation. ~~In fact, these~~These findings can be used to implement an advance-EWS-~~ warning system~~ based on the monitoring of a hydrometeorological process to issue a warning before a possible lahar is triggered.

Acknowledgements.

This work was supported by CONACyT projects 230 and 220786 granted to Lucia Capra and by the postdoctoral fellowship of DGAPA (Programa de Becas Posdoctorales de la UNAM) granted to Velio Coviello. Thanks to José Luis Ortiz and Sergio Rodríguez, from the Centro de Prevención de Desastres (CENAPRED), who set up the instrumentation on the Montegrande monitoring site.

References

Aleotti P (2004) A warning system for rainfall-induced shallow failures. Eng. Geol. 73(3-4): 247–265.

Barclay J, Alexander J, Susnik L (2007) Rainfall-induced lahars in the Belham valley, Monserrat, West Indies. Journal of the Geological Society of London 164: 815-827.

Bartolini D, Borselli L (2009) Evaluation of the HydrologicSoil Group (HSG) with the Procedure SCS Curve Number. *In*: Manualof Methods for Soil and Land Evaluation, Edoardo A, Costantini C (ed), Science Publisher Inc., 600 pages. ISBN 978-1-57808-571-2

Baum R L, Godt JW (2009) Early warning of rainfall-induced shallow landslides and debris flows in the USA. Landslides 7(3): 259–272.

Bendjoudi H, Hubert P (2002) Le coefficient de Gravélius : analyse critique d'un indice de forme des bassins versants. J. Sci. Hydrol. 47: 921–930.

Capra L, Borselli L, Varley N, Norini G, Gavilanes-Ruiz JC Sarocchi D, Caballero L (2010) Rainfall-triggered lahars at Volcán de Colima, Mexico: surface hydro-repellency as initiation process. Journal of Volcanology and Geothermal Research 189(1-2): 105-117.

Capra L, Macias JL, Cortes A, Saucedo S, Osorio-Ocampo S, Davila N, Arce JL, Gavilanes-Ruíz JC, Corona-Chávez P, García-Sánchez L, Sosa-Ceballos G, Vázquez R (2016) Preliminary report on the July 10-11, 2015 eruption at Volcán de Colima: Pyroclastic density currents with exceptional runouts and volumes. Journal of Volcanology and Geothermal Research 310: 39-49.

Con formato: Espacio Antes: 12 pto

Con formato: Fuente: Cursiva

Con formato: Espacio Antes: 12 pto, Interlineado: 1.5 líneas

Con formato: Español (México)

Con formato: Espacio Antes: 12 pto

Chen L, Xiang L, Young MH, Yin J, Yu Z, van Genuchten MT (2015) Optimal parameters for the Green-Ampt infiltration model under rainfall conditions. J. Hydrol. Hydromech. 63(2): 93–101

Chong S K, Teng T M (1986) Relationship between the runoff curve number and hydrologic soil properties. J. Hydrol. 84(1–2): 1–7.

Cortes A, Macias JL, Capra L, Garduño-Monroy VH (2010) Sector collapse of the SW flank of Volcán de Colima, México. The 3600 yr BP La Lumbre-Los Ganchos debris avalanche and associated debris flows. Journal of Volcanology and Geothermal Research 197: 52-66.

Coviello V, Capra L, Vázquez R, Marquez-Ramirez V, under revision. Seismic characterization of hyperconcentrated flows in volcanic environment. Earth Surface Processes and Landforms.

~~Cronin SJ, Hodgson KA, Neall VE, Palmer AS, Lecointre JA (1997) 1995 Ruapehu lahars in relation to the late Holocene lahars of Whangaehu River, New Zealand. New Zealand Journal of Geology and Geophisics 40: 507-520.~~

Davila N, Capra L, Gavilanes JC, Varley N, Norini G (2007) Recent lahars at Volcán de Colima (Mexico): drainage variation and spectral classification. Journal of Volcanology and Geothermal Research 165: 127-141.

de Bélizal E, Lavigne F, Hadmoko DS, Degai JP, Dipayana GA, Mutagin BW, Marfai MA, Coquet M, Le Mauff B, Robin AK, Vidal C, Cholik N, Aisyah N (2013) Rain-triggered

Con formato: Justificado, Espacio Antes: 12 pto, Interlineado: Doble

Con formato: Espacio Antes: 12 pto

lahars following the 2010 eruption of Merapi volcano, Indonesia: A major risk. Journal of Volcanology and Geothermal Research 261: 330-347.

Doyle EE, Cronin SJ, Cole SE, Thouret JC (2010) The coalescence and organization of lahars at Semeru volcano, Indonesia. Bulletin of Volcanology 72(8): 961-970.

Dumaisnil C, Thouret JC, Chambon G, Doyle EE, Cronin SJ (2010) Hydraulic, physical and rheological characteristics of rain-triggered lahars at Semeru volcano, Indonesia. Earth and Surface Processes and Landform 35: 1573-1590.

Ferrer-Julia~~o~~ M, Estrela T, Sanchez del Corral Jimenez A, Garcia-Melendez E (2003) Generation of a curve number map with continuous values based on saturated hydraulic conductivity. XI World Water Congress, 5-9 October 2003, Madrid, Spain: 1-10. http://iwra.org/member/index.php?mainpage=&page=286&congressyear=2003

Gentile F, Bisantino T, Puglisi S, Trisorio Liuzzi G (2006) Analysis and modeling of debris flows in Gargano watersheds (Puglia region, Southern Italy). WIT Transactions on Ecology and the Environment 90: 181-191.

Gravelius II (1914) Grundrifi der gesamten Gewcisserkunde. Band I: Flufikunde (Compendium of Hydrology, vol. I. Rivers, in German). Goschen, Berlin, Germany.

Greco R, Pagano L (2017) Basic features of the predictive tools of early warning systems for water-related natural hazards: examples for shallow landslides. Nat. Hazards Earth Syst. Sci., 17, 2213-2227, https://doi.org/10.5194/nhess-17-2213-2017, 2017

Green, W.H. and G. Ampt. 1911. Studies of soil physics, part I –the flow of air and water through soils. J. Ag. Sci. 4:1-24..

Con formato: Justificado, Espacio Antes: 12 pto, Interlineado: Doble, Diseño: Claro

Código de campo cambiado

Con formato: Fuente: Times New Roman, 12 pto, Sin Negrita, Sin subrayado, Color de fuente: Automático

Con formato: Fuente: Times New Roman, 12 pto, Color de fuente: Automático

Con formato: Fuente: Times New Roman, 12 pto

Con formato: Espacio Antes: 12 pto

Grimaldi S, Petroselli A, Romano N (2013) Green-Ampt Curve-Number mixed procedure as an empirical tool for rainfall–runoff modelling in small and ungauged basins. Hydrol. Process. 27: 1253–1264

Hawkins RH, Hjelmfelt AT, Zevenbergen AW (1985) Runoff probability storm depth and curve numbers. Journal of the Irrigation and Drainage Division 111: 330-340.

Kean W, McCoy S, Tucker G, Staley D, Coe J (2013) Runoff-generated debris flows: Observations and modeling of surge initiation, magnitude, and frequency. Journal of Geophysical Research: Earth Surface 118: 1-18.

Keefer DK, Wilson RC, Mark RK, Brabb EE, Brown WM, Ellen SD, Harp EL, Wieczorek, GF, Alger CS, Zatkin RS (1987) Real-time landslide warning during heavy rainfall. Science 238(4829): 921–5.

Jones R, Manville V., Peakall J, Froude MJ, Odbert HM. (2017) Real-time prediction of rain-triggered lahars: Incorporating seasonality and catchment recovery. Natural Hazards and Earth System Sciences 17(12): 2301-2312.

Jones R, Manville V, Andrade D (2015) Probabilistic analysis of rain-triggered lahar initiation at Tungurahua volcano. Bulletin of Volcanology 77(8): 68.

Iverson RM (1997) The physics of debris flows: Reviews of Geophysics 35: 245-296.

Lavigne F, Thouret JC, Voight B, Suwa H, Sumaryono A (2000) Lahars at Merapi volcano, Central Java: an overview. Journal of Volcanology and Geothermal Research 100: 423-456.

Con formato: Sin subrayado, Color de fuente: Automático

Con formato: Justificado, Espacio Antes: 12 pto, Interlineado: Doble

Código de campo cambiado

Con formato: Sin subrayado, Color de fuente: Automático

Código de campo cambiado

Con formato: Fuente de párrafo predeter.

Código de campo cambiado

Con formato: Sin subrayado, Color de fuente: Automático

Código de campo cambiado

Con formato: Sin subrayado, Color de fuente: Automático

Código de campo cambiado

Con formato: Sin subrayado, Color de fuente: Automático

Código de campo cambiado

Con formato: Sin subrayado, Color de fuente: Automático

Con formato: Sin subrayado, Color de fuente: Automático

Código de campo cambiado

Con formato: Sin subrayado, Color de fuente: Automático

Código de campo cambiado

Con formato: Sin subrayado, Color de fuente: Automático

Código de campo cambiado

Código de campo cambiado

Con formato: Sin subrayado, Color de fuente: Automático

Con formato: Espacio Antes: 12 pto

Lavigne F, Thouret JC (2002) Sediment transport and deposition by rain-triggered lahars at Merapi Volcano, Central Java, Indonesia. Geomophology 49: 45-69.

Llanes F, Ferrer PK, Gacusan R, Realino V, Obrique J, Eco RN, Lagmay AMF (2015) Scenario-based maps using flo-2d and IFSAR-derived digital elevation models on the November 2006 rainfall-induced lahars, Mayon Volcano, Philippines. ACRS 2015 Proceedings, Asian Association on Remote Sensing.

Marchi L, Arattano M, Deganutti A. (2002) Ten years of debris-flow monitoring in the Moscardaro Torrent (Italian Alps), Geomorphology 46: 1–17, doi:10.1016/S0169-555X(01)00162-3.

Mishra S K, Singh VP (2003) Soil conservation service curve number (SCS-CN) methodology. Kluwer Academic Publishers, Dordrecht, Netherlands.

Mockus V (1972) Estimation of direct runoff from storm rainfall national engineering handbook, Soil Conservation Service, Washington, DC.

NRCS-Natural Resource Conservation Services (2008) Rainfall-Frequency and Design Rainfall Distribution for Selected Pacific Islands. Engineering Technical Note No. 3, United States Department of Agriculture:115 pp.

O'Brien J, Julien P, Fullerton W (1993) Two-dimensional water flood and mudflow simulation. J. Hydraul. Eng.-ASCE 119: 244-261.

Con formato: Justificado, Espacio Antes: 12 pto, Interlineado: Doble

Con formato: Espacio Antes: 12 pto

Ortiz A. (2017) Modelado de conectividad y contribución de escorrentía superficial lateral en la dinámica de flujos granulares de áreas volcánicas activas. PhD thesis, Universidad Autónoma de San Luis Potosí, Facultad de Ciencias, México: 224 pp.

Ortiz-Rodríguez AJ, Borselli L, Sarocchi D (2017) Flow connectivity in active volcanic áreas: use of index of connectivity in the assessment of lateral flow contribution to main streams. Catena 157: 90 – 111.

Ponce V, Hawkins R (1996) Runoff curve number: Has it reached maturity? J. Hydrol. Eng. 1(11): 11–19.

Rallison RE (1980) Origin and evolution of the SCS runoff equation. In: Proc. ASCE Irrigation and Drainage Div. Symp. on Wathershed Management, vol. II. ASCE: New York, NY; 912–924.

Roverato M, Capra L, Sulpizio R, Norini G (2011) Stratigraphic reconstruction of two debris avalanche deposits at Colima Volcano (Mexico): Insights into pre-failure conditions and climate influence. Journal of Volcanology and Geothermal Research 207: 33-46.

Scott KM, Vallance JV, Kerle N, Macias JL, Strauch W, Devoli G (2005) Catastrophic precipitation-triggered lahars at Casita Volcano, Nicaragua: occurrence, bulking and transformation. Earth Surface Processes and Landforms 30: 59-79.

Sheridan MF, Connor CB, Connor L, Stinton AJ, Galacia O, Barrios G (2007) October 2005 Debris Flows at Panabaj, Guatemala: Hazard Assessment. American Geophysical Union, Spring Meeting 2007, abstract #V33A-07.

Con formato: Justificado, Espacio Antes: 12 pto, Interlineado: Doble

Con formato: Espacio Antes: 12 pto

Takahashi T (2007) Debris Flow: Mechanics Prediction, and Countermeasures. Taylor and Francis/Balkema, Leiden: 448 pp.

Umbal JV, Rodolfo KS (1996) The 1991 lahars of southwestern Mount Pinatubo and evolution of the lahar-dammed Mapanuepe lake. Fire and mud; eruptions and lahars of Mount Pinatubo, Philippines, P. I. o. V. a. Seismology, ed., Quezon, Philippines: pp. 951-970.

USDA-NRCS (U.S. Department of Agriculture-Natural Resources Conservation Service). (2007) Hydrologic soil groups. National engineering handbook. Part 630 hydrology, Washington, DC.

van Westen CJ, Daag AS (2005) Analysing the relation between rainfall characteristics and lahar activity at Mount Pinatubo, Philippines. Earth and Surface Processes and Landform 30: 1663-1674.

Van Wyk Vries B, Kerle N, Petley D (2000) Sector collapse forming at Casita volcano, Nicaragua. Geology 28(2): 167-170.

Vázquez R, Suriñach E, Capra L, Arámbula-Mendoza R, Reyes-Dávila G (2016a) Seismic characterisation of lahars at Volcán de Colima, Mexico. Bulletin of Volcanology 78: 8.

Vázquez R, Capra L, Coviello V (2016b) Factors controlling erosion/deposition phenomena related to lahars at Volcán de Colima, Mexico. Natural Hazards and Earth System Sciences 16: 1881–1895.

Wei L-W, Huang C-M, Lee C-T, Chi C-C, Chiu C-L (2017) Adopting I_3–R_{24} rainfall index and landslide susceptibility on the establishment of early warning model for rainfall-

Con formato: Justificado, Espacio Antes: 12 pto, Interlineado: Doble

Código de campo cambiado

Con formato: Fuente: Times New Roman, 12 pto, Sin Negrita, Sin subrayado, Color de fuente: Automático

induced shallow landslides. Nat. Hazards Earth Syst. Sci. Discuss., https://doi.org/10.5194/nhess-2017-428, 2017.

Zanuttigh B, Lamberti A (2007) Instability and surge development in debris flows. Rev. Geophys. 45: RG3006, doi:10.1029/2005RG000175.

Zobin VM, Placencia I, Reyes G, Navarro C (2009) The characteristics of seismic signal produced by lahars and pyroclastic flows: Volcán de Colima, Mexico. Journal of Volcanology and Geothermal Research 179: 157-167.

Con formato: Color de fuente: Automático

Con formato: Espacio Antes: 12 pto

Figure captions

Figure 1. a) Aster image (4, 5 and 7 bands in RGB combination) where main watersheds at Volcán de Colima are represented. The locations of the monitoring stations are indicated. The inset shows the location of the rain gauge of the Meteorological National Service at the summit of the Nevado de Colima Volcano. b) Sketch map of the Trans Mexican Volcanic Belt (TMVB) and the Volcán de Colima location. Black triangles denote the main active volcanoes in México

Figure 2. a) Panoramic view of the Volcán de Colima showing the unvegetated main cone mostly composed by loose volcanic fragments. b) Montegrande and c) La Lumbre ravines in the middle reach where it is possible to observe the main channel flanked by 10-15m-high terraces mainly constituted by debris avalanche deposits.

Figure 3. a) Cumulative values of rainfall of hurricanes Jova, Manuel and Patricia calculated at 10 min-intervals; ~~a~~b) Normalized rainfall curves for the Jova and Patricia events as gathered from two different stations, pointing to a quasi-stationary rainfall behavior;~~.~~ ~~ab) Cumulative and~~ c~~b~~) normalized values of cumulative rainfall curves ~~of rainfall of hurricanes Jova, Manuel and Patricia calculated at 10 min-intervals~~. d~~c~~) Normalized curve of total rainfalls cumulated at 15, 30, 60 minutes and 1, 3, 6, 12, 18, 24, 28 hrs. Dotted line represents the average value between Manuel and Patricia hurricanes.

Figure 4. Comparison of simulated watershed discharge curves based on SCS-NC and G-A infiltration models. Qualitative calibration is here proposed based on the flow discharge as observed in the video images captured at the MSL site.

Figure 5~~4~~. a) Seismic record of the lahar triggered during the Hurricane Jova, on 12 October, 2011. b) Seismic record of the lahar triggered during the 11 June, 2013 events. Main pulses are indicated with roman letters. c) Images captures by the camera corresponding to the main lahar pulses as indicated in figure b.

Figure 6~~5~~. Images showing the morphology of the channel at the monitoring site of the Montegrande ravine, a) the day before and b) the day after the Hurricane Jova~~. c) Topographic profiles showing that the channel was eroded 1.5 m in depth.~~.

Figure 7~~6~~. Seismic record of the lahar triggered during the Hurricane Manuel, on 15 September, 2013, recorded along the Montegrande ravine

Figure 8~~7~~. a) Seismic record of the lahar triggered during the Hurricane Patricia, on 26 October, 2015, recorded along the La Lumbre ravine. Main lahar pulses are indicated with roman letters. b) Images captured by the camera corresponding to the main pulses as indicated in figure a.

Figure 9~~8~~. Diagrams showing the main lahar pulses (red triangles) as detected from the seismic signal of the analyzed events in relation with the accumulated rainfall (dark line), rainfall intensity (10m/hr) (gray line) and simulated watershed discharge (blue line) for the following hidrometeorological events a) Jova; b) Manuel; c) 13 June, 2013; and d) Patricia.

Table 1. Data collected for the events here studied.

Table 2. Normalized accumulated rains ~~(in percentage)~~ at progressive time steps.

Table 3. Parameters used in the G-A simulations

Con formato: Fuente: Sin Negrita, Sin Cursiva

Table 4. Arrival times of peak III and IV using different CN values.

Table 1. Data collected for the events here studied.

Event	**ravine**	**Seismic record**	**Image record**	**Rain gauge**	**Total rain (mm)**	**Max. rain intensity (mm/hr)**
Jova, 12~~1~~/10/2011	Montegrande	X		MSMg	240	43
Manuel 15/09/2013	Montegrande	X		MSMg	300	32
Patricia 23/10/2015	Lumbre	X	X	NS	400	37
11 June 2013	Montegrande	X	X	MSMg	120	140

Table 2. Normalized accumulated rains ~~(in percentage)~~ at progressive time steps.

Event/time (hrs)	0.25	0.5	1	2	3	6	12	24	27
Jova	0.0011	0.0016	0.0035	0.0172	0.0329	0.1411	0.7073	0.968	0.9943
Manuel	0.0023	0.0035	0.0042	0.0072	0.0151	0.0341	0.1548	0.735	0.9181
Patricia	0.0002	0.0004	0.0009	0.0062	0.0174	0.0556	0.2544	0.829	0.9782
Average	***0.00125***	***0.00195***	***0.00255***	***0.0067***	***0.01625***	***0.04485***	***0.2046***	***0.782***	***0.9481***

The average values refer to hurricanes Manuel and Patricia.

Table 3. Parameters used in the G-A simulations

Abstraction	6 mm
Ks	20 mm/hr
soil-suction	100 mm
initial saturation	0.1
final saturation	0.35

Con formato: Fuente: Sin Negrita, Sin Cursiva

Tabla con formato

Con formato: Izquierda

Con formato: Izquierda

Table 4. Arrival times~~Time arrival~~ of peak III and IV using defferent CN values.

Surges observed in the images	**peak III (23.5 hr)**	**peak IV (24 hr)**
CN	*Arrival times (hr) in the simulated watershed discharge curves*	
75 global	23.4	24.1
80/75 (channel/vegetated)	23.5	24.1
80 global	23.5	24.2

Con formato: Fuente: Sin Negrita, Sin Cursiva

Con formato: Fuente: Sin Negrita, Sin Cursiva

Con formato: Fuente: Sin Negrita, Sin Cursiva

Tabla con formato

Con formato: Fuente: Sin Cursiva

Con formato: Fuente: Sin Negrita, Sin Cursiva

Con formato: Fuente: Sin Negrita, Sin Cursiva

Con formato: Fuente: Sin Negrita, Sin Cursiva

Con formato: Fuente: Sin Cursiva

Fig. 01

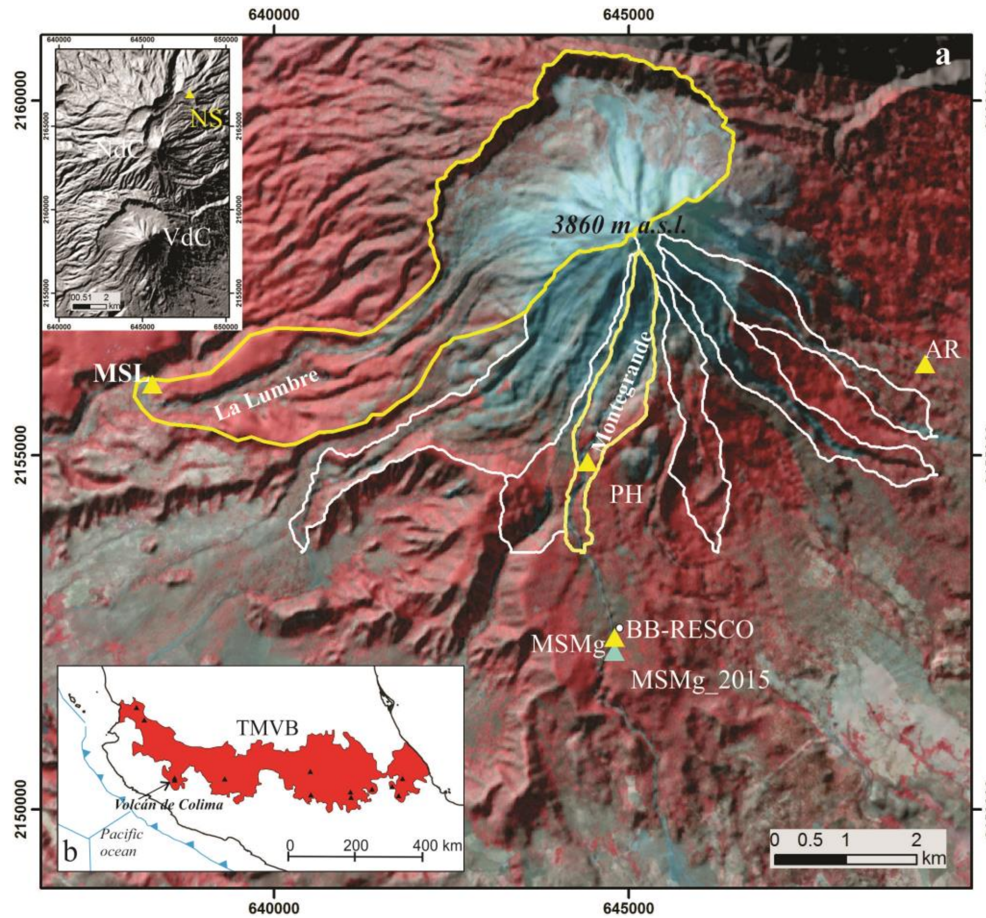
640000
645000
a
2160000
2155000
2150000
NS
NdC
VdC
3860 m a.s.l.
AR
MSL
La Lumbre
Montegrande
PH
BB-RESCO
MSMg
MSMg_2015
TMVB
Volcán de Colima
Pacific ocean
b
0 200 400 km
0 0.5 1 2 km

Fig. 02

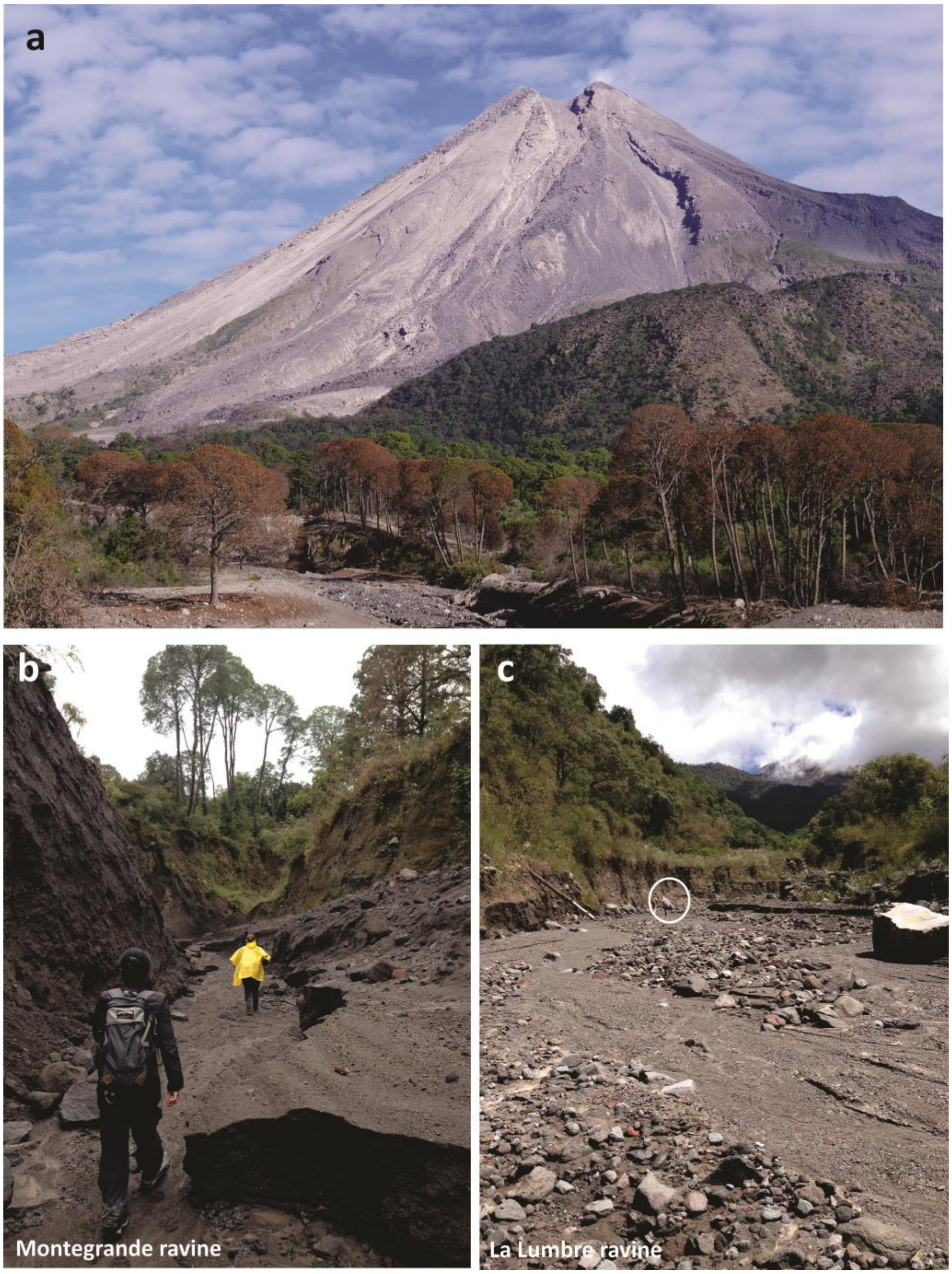

Fig- 03

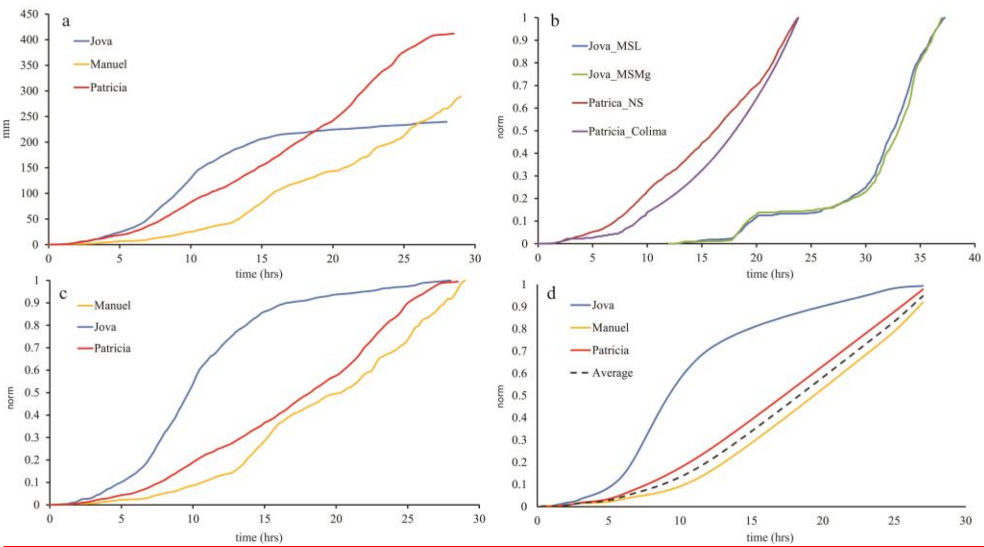

a
Jova
Manuel
Patricia
mm
time (hrs)
b
Jova_MSL
Jova_MSMg
Patrica_NS
Patricia_Colima
norm
time (hrs)
c
Manuel
Jova
Patricia
norm
time (hrs)
d
Jova
Manuel
Patricia
Average
norm
time (hrs)

Fig. 04

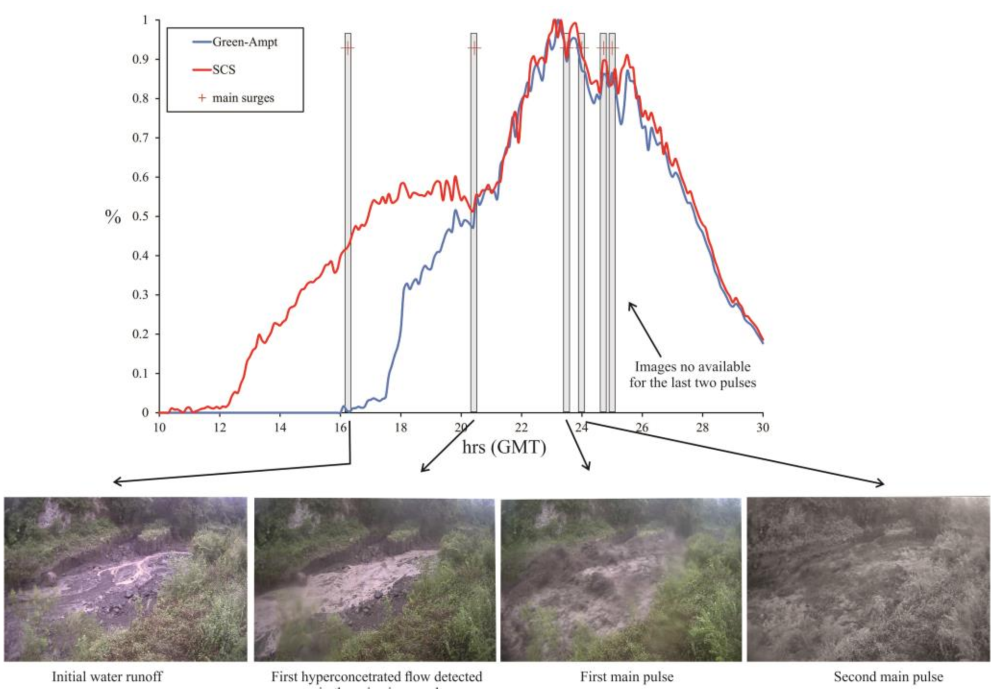

Green-Ampt
SCS
main surges
%
hrs (GMT)
Images no available
for the last two pulses
Initial water runoff
First hyperconcetrated flow detected
in the seismic record
First main pulse
Second main pulse

Fig. 054

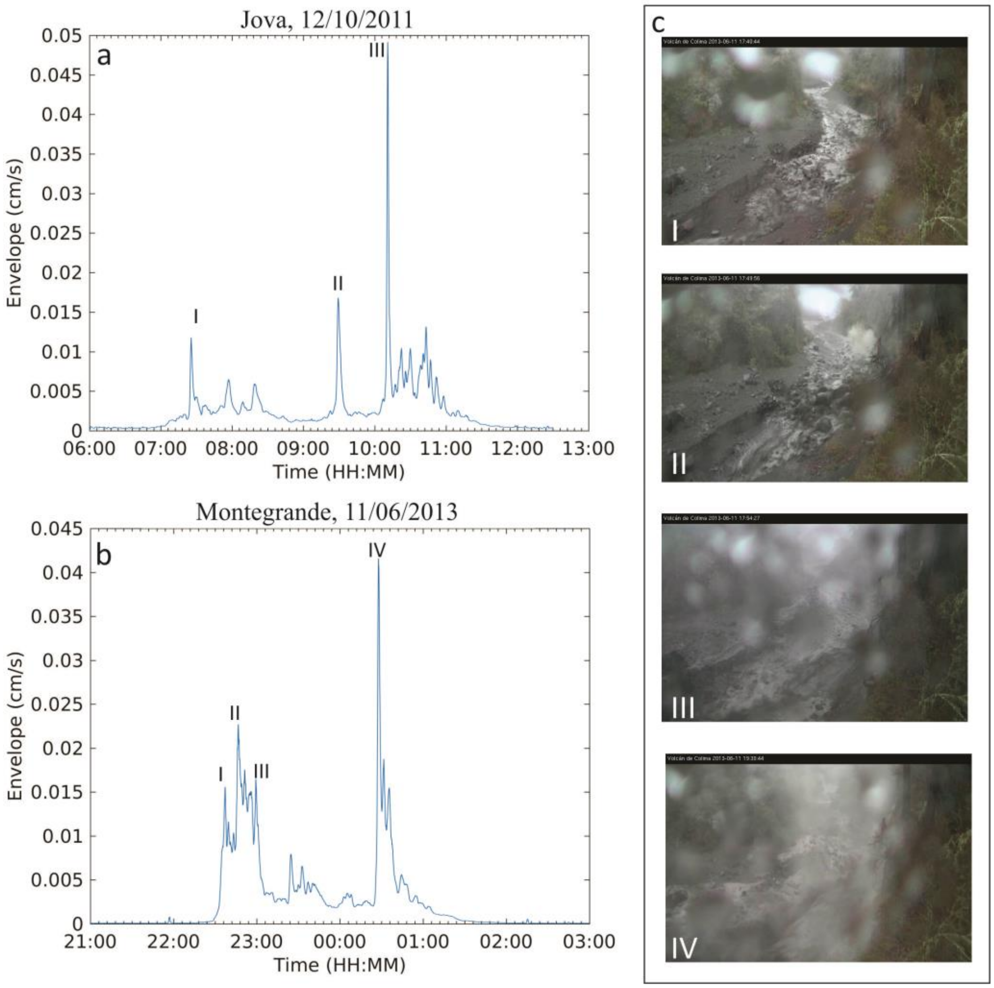
Jova, 12/10/2011
a
I
II
III
Envelope (cm/s)
Time (HH:MM)
Montegrande, 11/06/2013
b
I
II
III
IV
Envelope (cm/s)
Time (HH:MM)
c
I
II
III
IV

Fig. 056

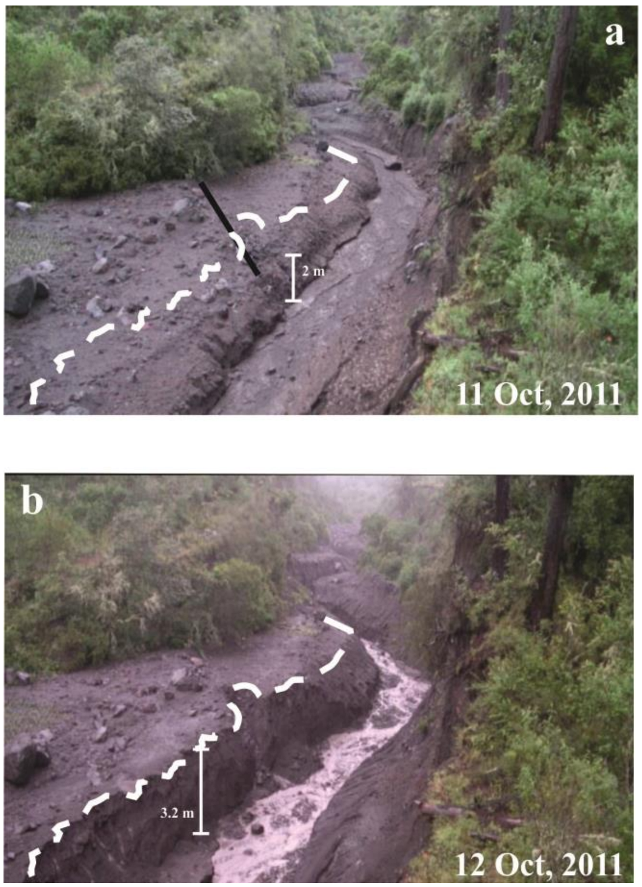

Fig. 076

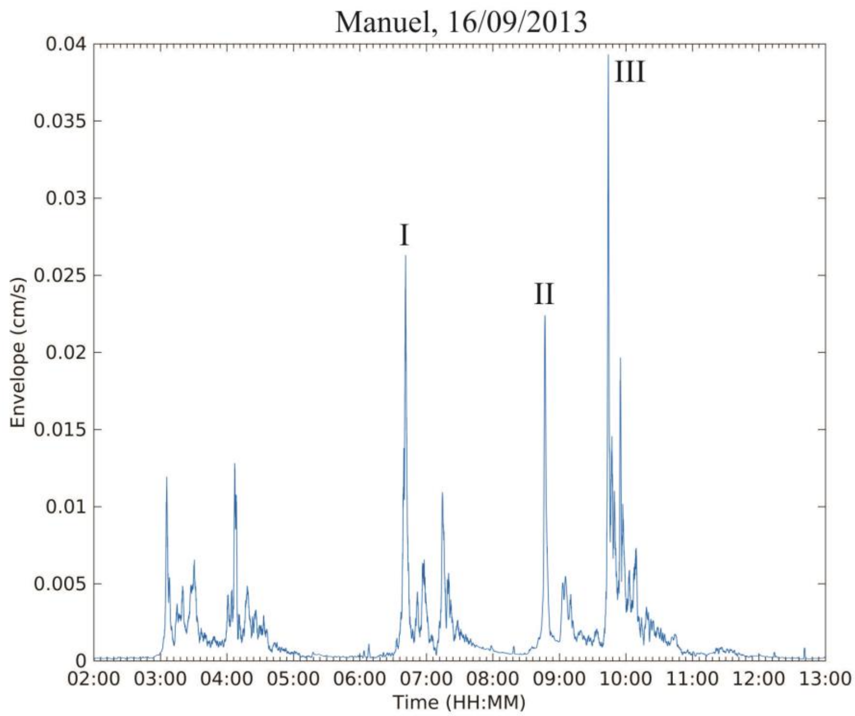
Manuel, 16/09/2013
Envelope (cm/s)
Time (HH:MM)
I
II
III
0
0.005
0.01
0.015
0.02
0.025
0.03
0.035
0.04
02:00
03:00
04:00
05:00
06:00
07:00
08:00
09:00
10:00
11:00
12:00
13:00

Fig. 087

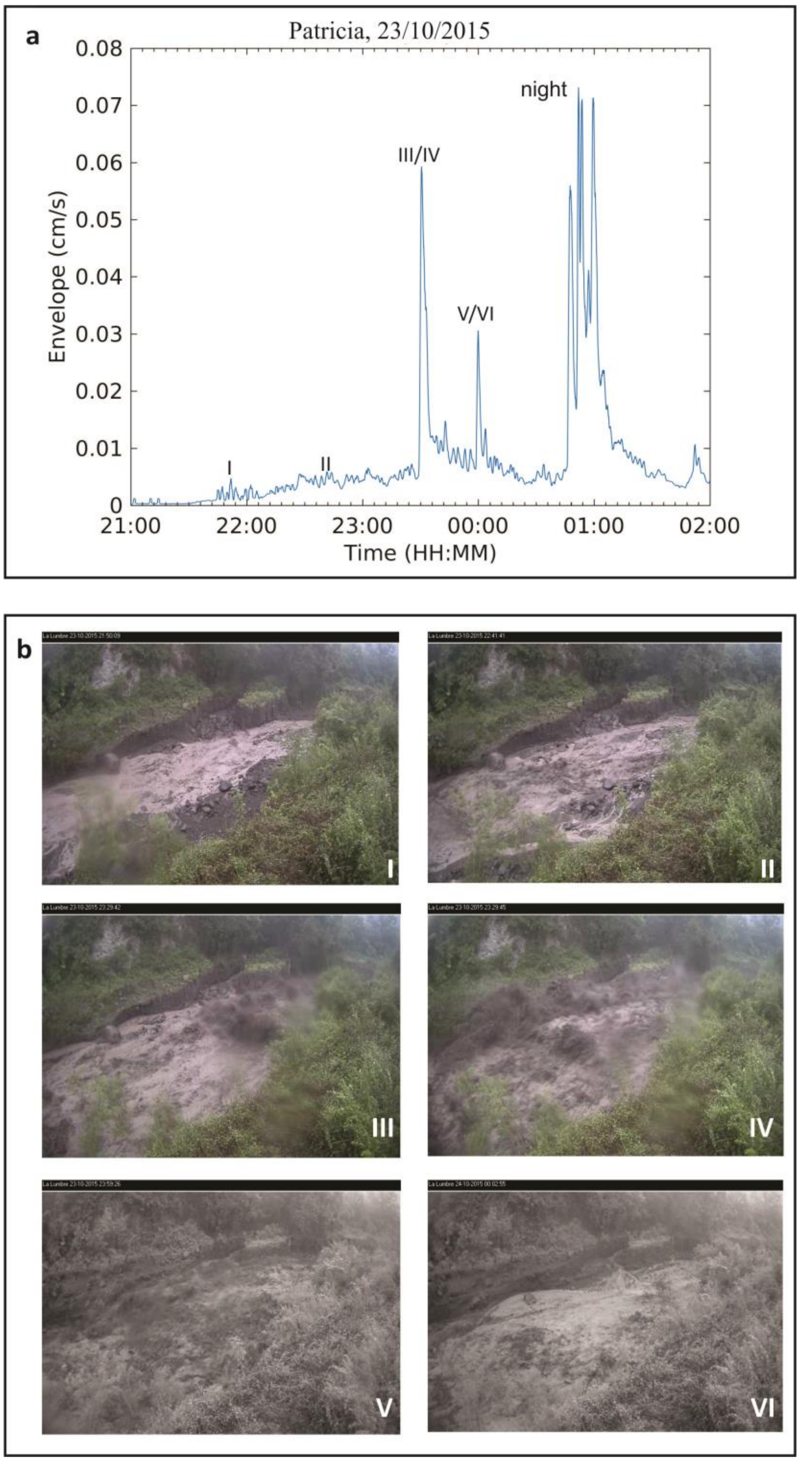
a
Patricia, 23/10/2015
Envelope (cm/s)
Time (HH:MM)
0.08
0.07
0.06
0.05
0.04
0.03
0.02
0.01
0
21:00
22:00
23:00
00:00
01:00
02:00
I
II
III/IV
V/VI
night
b
I
II
III
IV
V
VI

Fig. 098

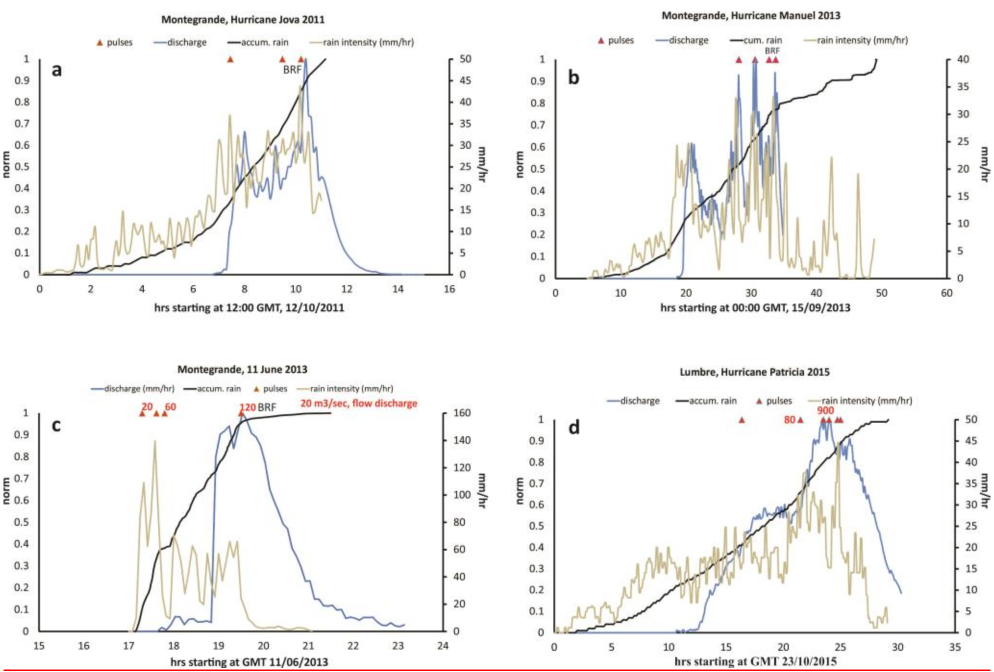
Montegrande, Hurricane Jova 2011
pulses
discharge
accum. rain
rain intensity (mm/hr)
a
BRF
norm
mm/hr
hrs starting at 12:00 GMT, 12/10/2011
Montegrande, Hurricane Manuel 2013
pulses
discharge
cum. rain
rain intensity (mm/hr)
b
BRF
norm
mm/hr
hrs starting at 00:00 GMT, 15/09/2013
Montegrande, 11 June 2013
discharge (mm/hr)
accum. rain
pulses
rain intensity (mm/hr)
c
20
60
120
BRF
20 m3/sec, flow discharge
norm
mm/hr
hrs starting at GMT 11/06/2013
Lumbre, Hurricane Patricia 2015
discharge
accum. rain
pulses
rain intensity (mm/hr)
d
80
900
norm
mm/hr
hrs starting at GMT 23/10/2015